TECHNISCHE UNIVERSITÄT DARMSTADT

INSTITUTE FOR MATERIALS SCIENCE

Ion Beam Techniques

and their applications

Adam Georg Balogh
Institute for Materials Science
Technische Universität Darmstadt

Frequently used techniques of Ion Beam Analysis

	Primary ions	Signal to detect	E_P	Depth resolution	Spatial resolution
Methods:					
ERDA	Middle-heavy ions	Atoms from the target (1<Z<10)	ca. 1 MeV/amu	yes	no
PIXE	Protons	γ	1-3 MeV	no	possible
SIMS	O, Cs Ions	Charged atoms from the target	4-12 keV	yes	yes
NRA	Light ions	p, α, γ	0.2-10 MeV	yes	no
RBS	H^+, He^+, He^{++}	Projektiles	1-2 MeV	yes	no

Modification of surfaces and interfaces using heavy ions

ion implantation and/or irradiation

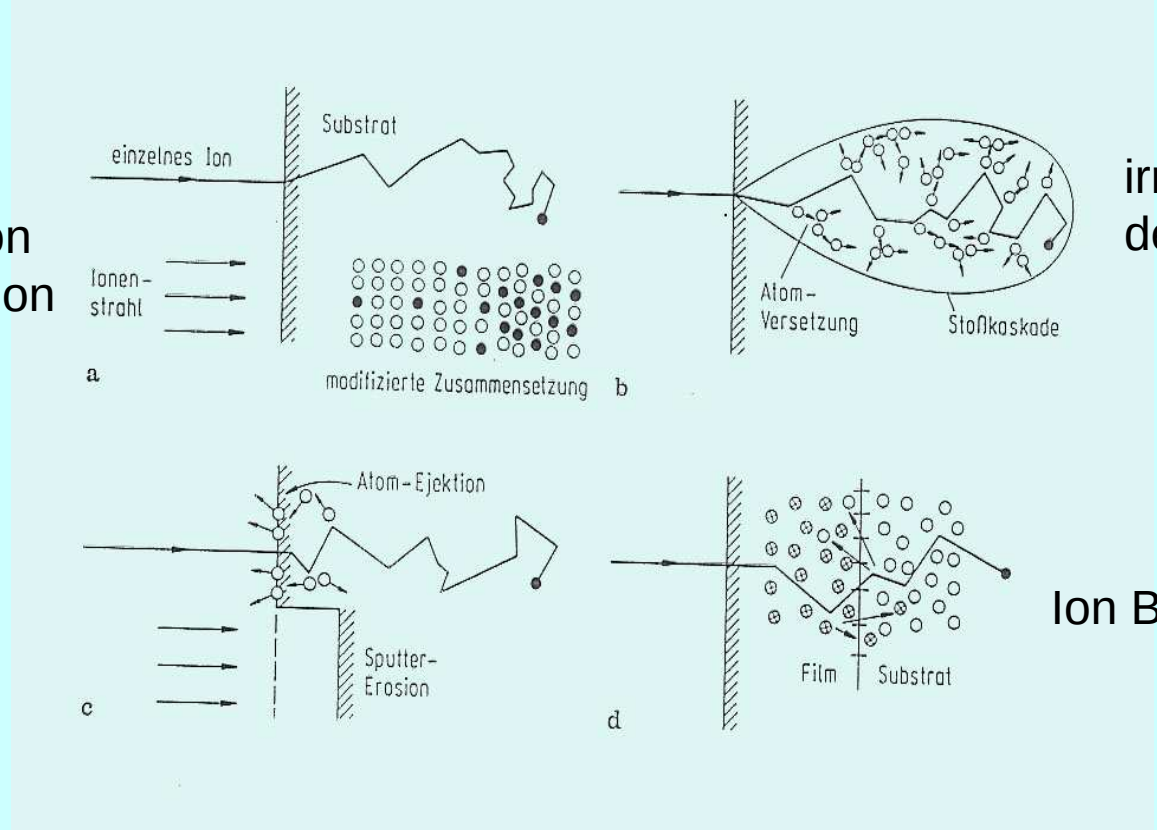

irradiation induced defects (cascades)

sputtering

Ion Beam Mixing (IBM)

Possibilities in Darmstadt-Frankfurt area

50 keV implanter for different gases and metals

2.5 MeV Van de Graaff accelerator for H, He, Ne, Ar, Kr ions
modification with nuclear energy loss and ion beam analysis

High energy beams at the GSI, Darmstadt (Institute for Heavy Ion Research)
modification with electronic energy loss

International Conference on „Materials Science Applications of Ion Beam Techniques“ organised already 1996 near Darmstadt
Proceedings, eds. A.G. Balogh, G. Walter, Trans Tech Publ., 1997

Rutherford Backscattering Spectrometry (RBS)

Elastic scattering of light ions on the Coulomb potential of the atomic nuclei.

First RBS measurement has been performed by Geiger und Marsden in 1913 in order to prove the new scattering theory of Rutherford.

First application:

analysis of the moon surface during the Surveyor V. mission in 1967 (Turkevich 1968), using the 6.1 MeV α-particles of a ^{242}Cm-Quelle

Diagrammatic set-up of the RBS measurements

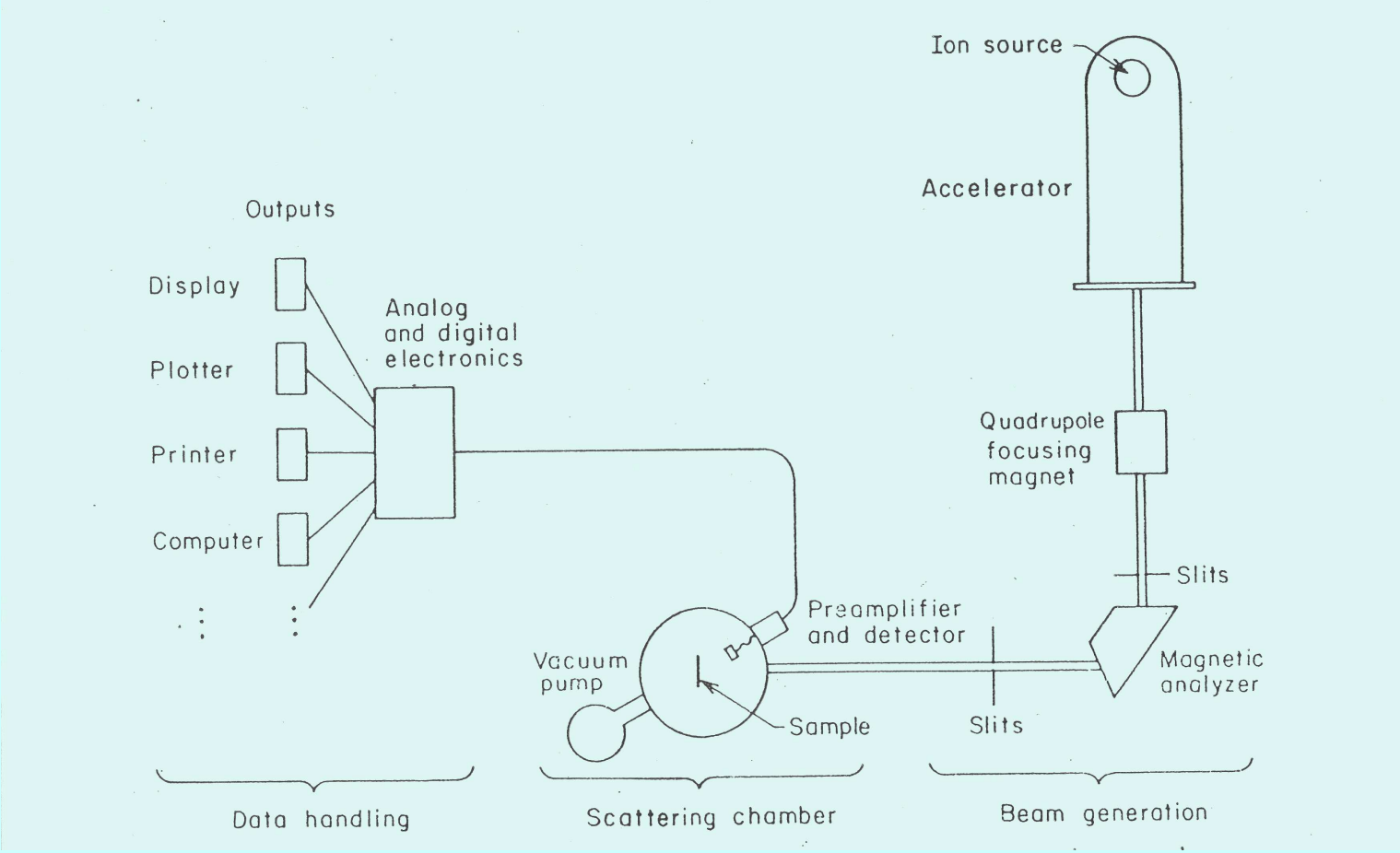

simplified view of a scattering chamber

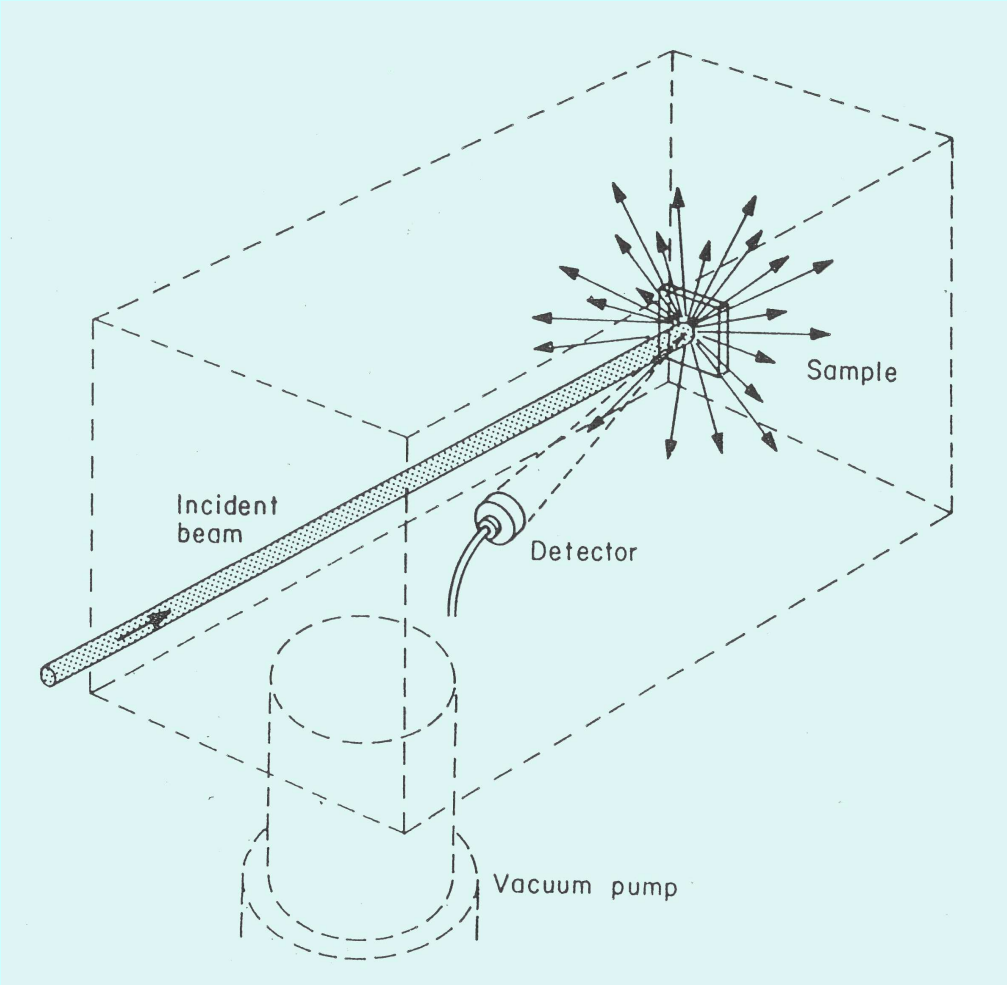

If the impact factor (distance between projectile and nucleus) is small enough, α - particles will be backscattered.

Because of the small impact factor the repulsive Coulomb potential is very strong ($F_c \sim 1/r^2$).

The energy of the backscattered particles will be determined by the kinematic factor:

$$K=E_1/E_0$$

with E_0 = 1 MeV:

K(Al) = 0.5527	E_1(Al) = 552.7 keV
K(Au) = 0.9225	E_1(Au) = 922.5 keV

RBS spectrum of a film-on-substrate sample

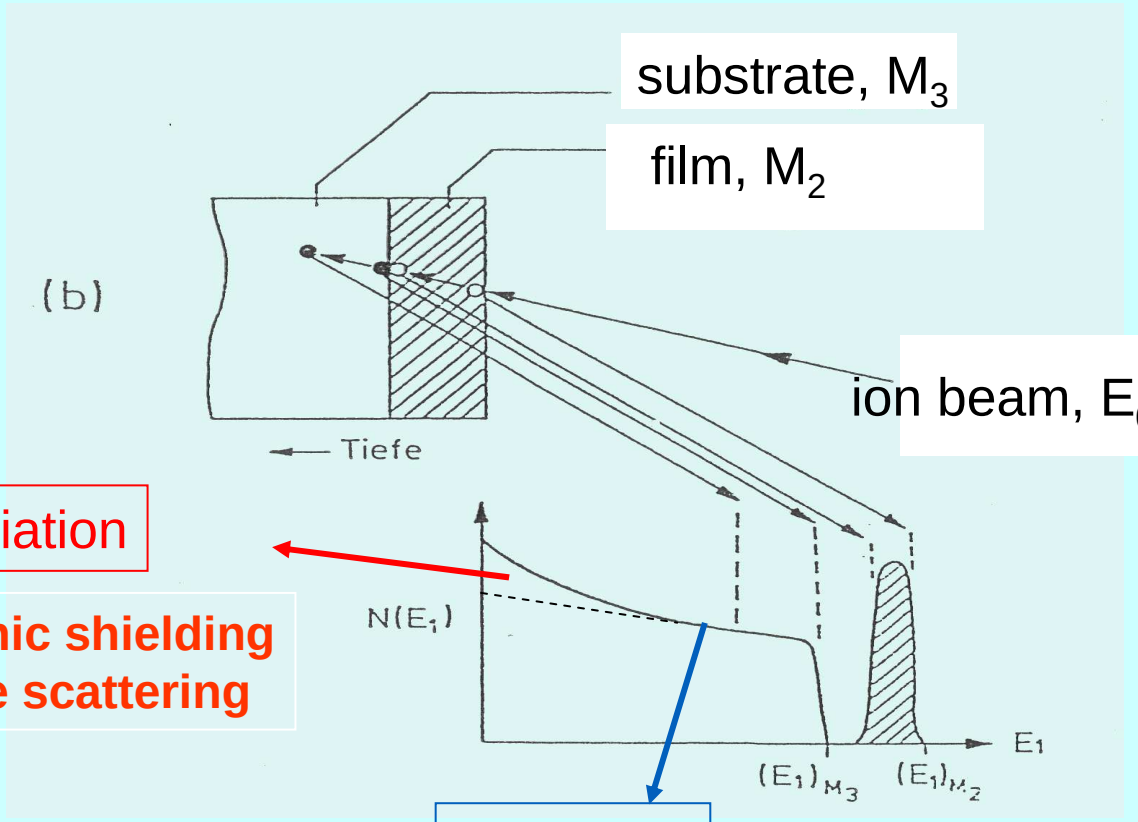

$$\sigma_R \approx 1/E^2$$

The Rutherford cross section

$$\sigma_R = \left(\frac{Z_1 Z_2 e^2}{4E}\right)^2 \frac{4}{\sin^4\Theta} \frac{\left\{\left[1-\left(\frac{m}{M}\sin\Theta\right)^2\right]^{1/2} + \cos\Theta\right\}^2}{\left[1-\left(\frac{m}{M}\sin\Theta\right)^2\right]^{1/2}}$$

Most important is the pre-factor:

$$\left(\frac{Z_1 Z_2 e^2}{4E}\right)^2$$

The Rutherfod cross section depends on the:
pre-faktor
mass ratio (m/M)
scattering angle (Θ)

$$\frac{\sigma_R}{\left(\frac{Z_1 Z_2 e^2}{4E}\right)^2} \approx \frac{m}{M}, \Theta$$

The dependence of the Rutherford differential scattering cross section as a function of the scattering angle θ and the mass ratio $x^{-1} = M_2/M_1$

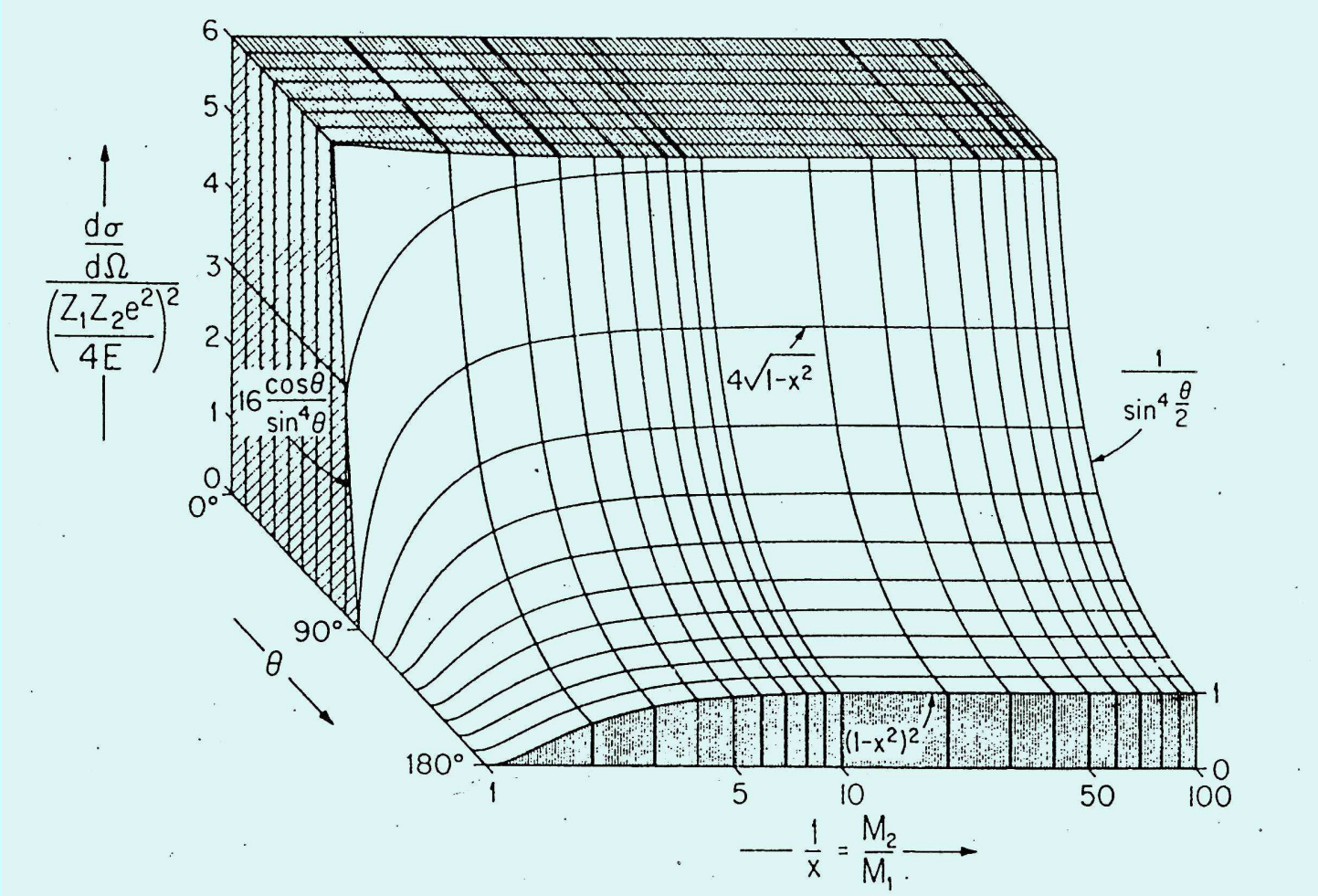

Intensity (counts in the RBS spectrum) is:

$$A = Q N t \sigma_R \Omega$$

Q – charge; σ_R – Rutherford cross section; Ω – detector solid angle

If they are known → Nt (mass density) is to define

This has the consequence that:

1. If the layer thickness is known, density can be determined
2. If the density is known, thickness can be determined

Mass sensitivity

To get a high mass sensitivity it is necessary that ΔM gives rise to a high ΔE_1:

$$\Delta E_1 = E_0 \left(4 - \delta^2\right) \left(m / M^2\right) \Delta M$$

possibilities:

- high primary energy
- heavy primary ion
- high scattering angle

Light element sensitivity at E=2 MeV

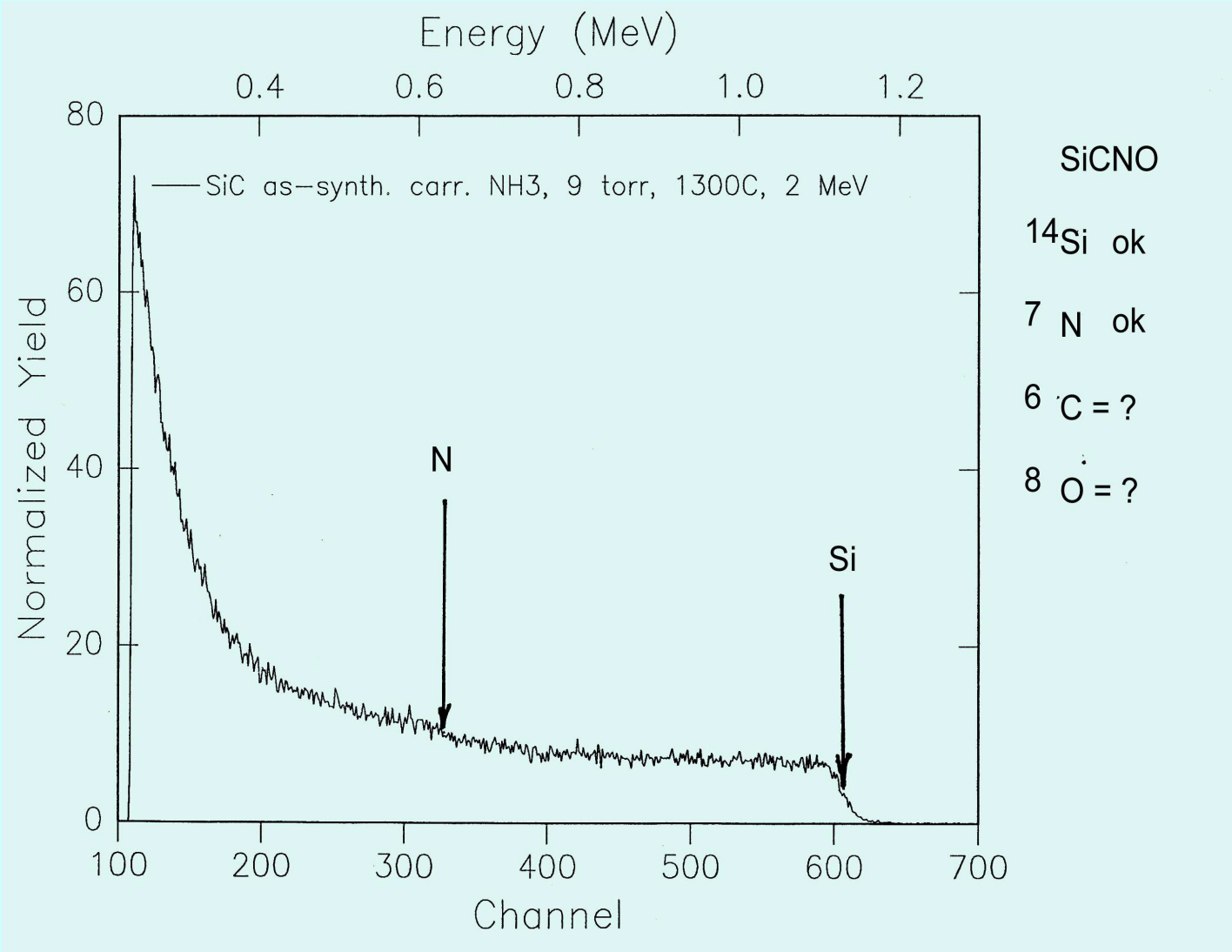

Increased sensitivity at 3.5 MeV

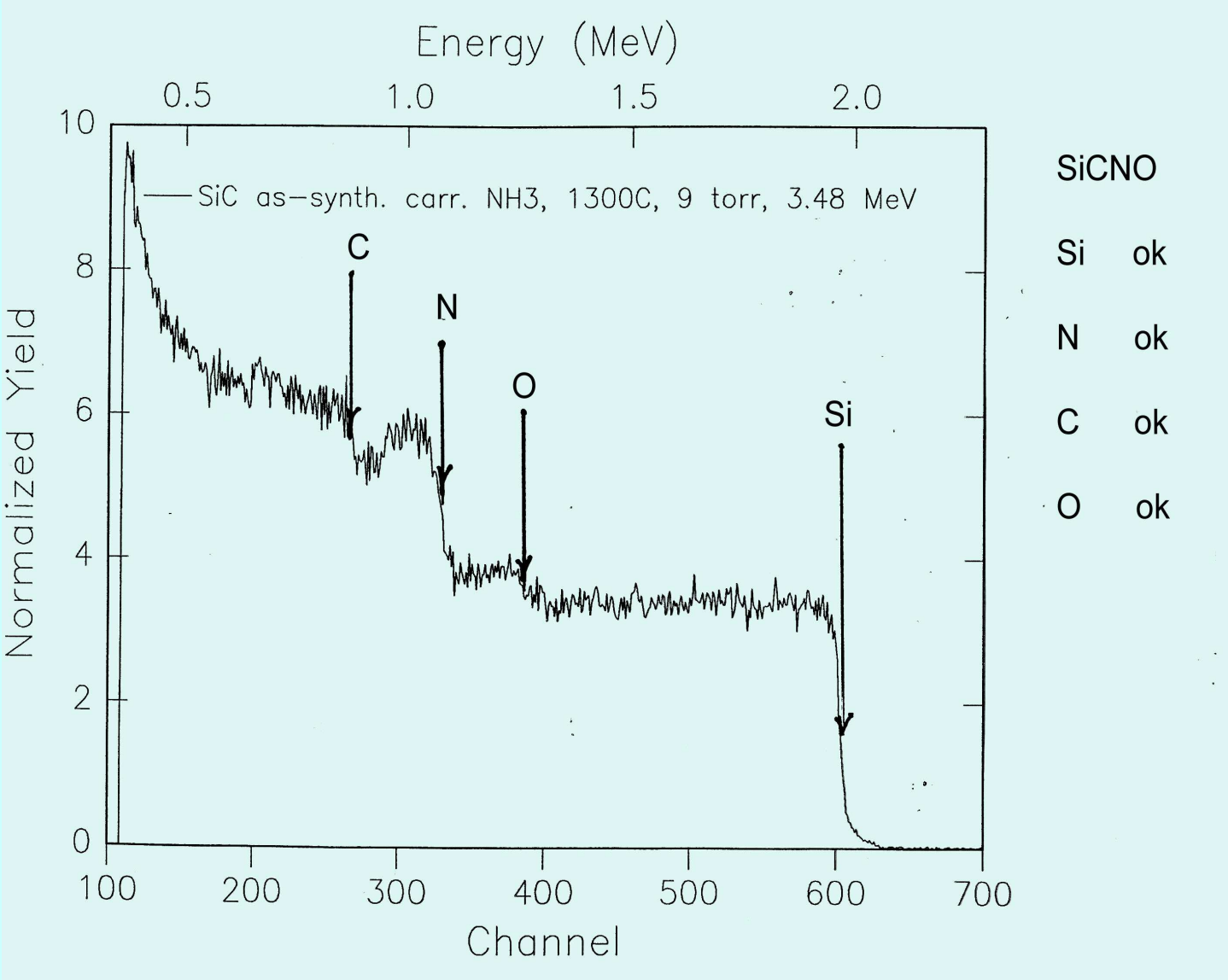

Resolution of thin Fe/Mo multilayers with 1.9 MeV He ions

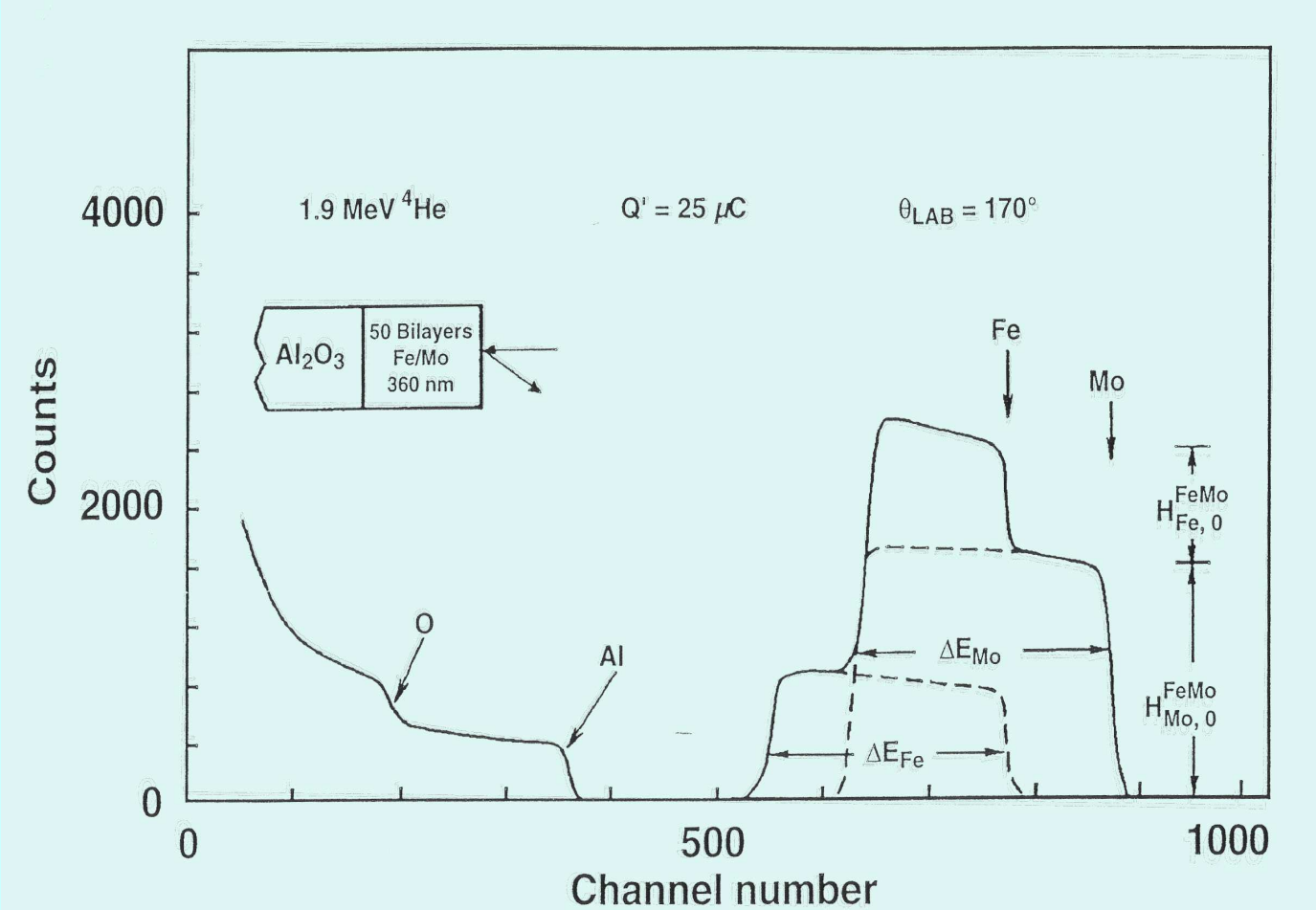

Increased resolution using 3.8 MeV He ions

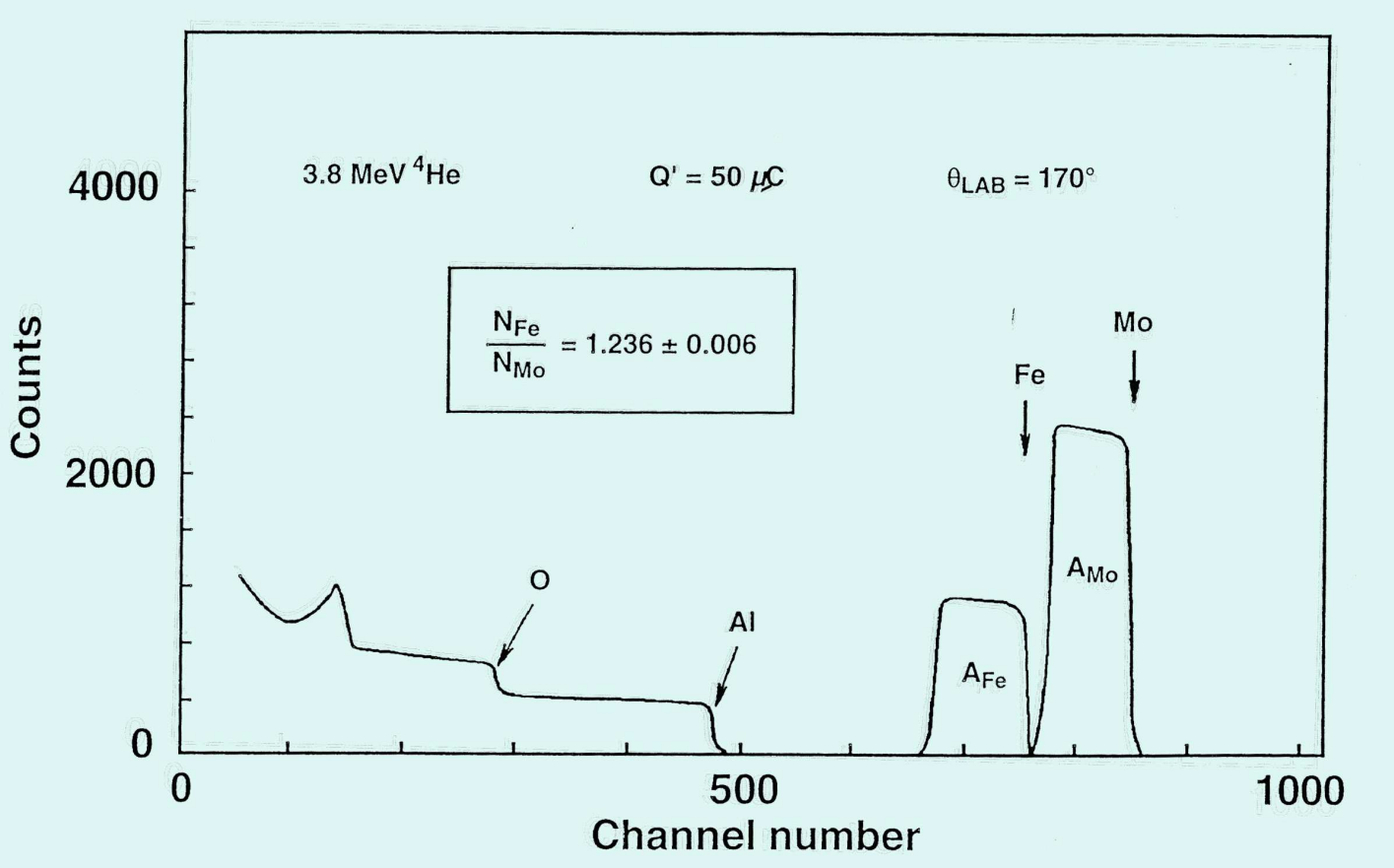

Dependence of the RBS spectrum of a high-Tc superconductor on the energy and on the primary ions

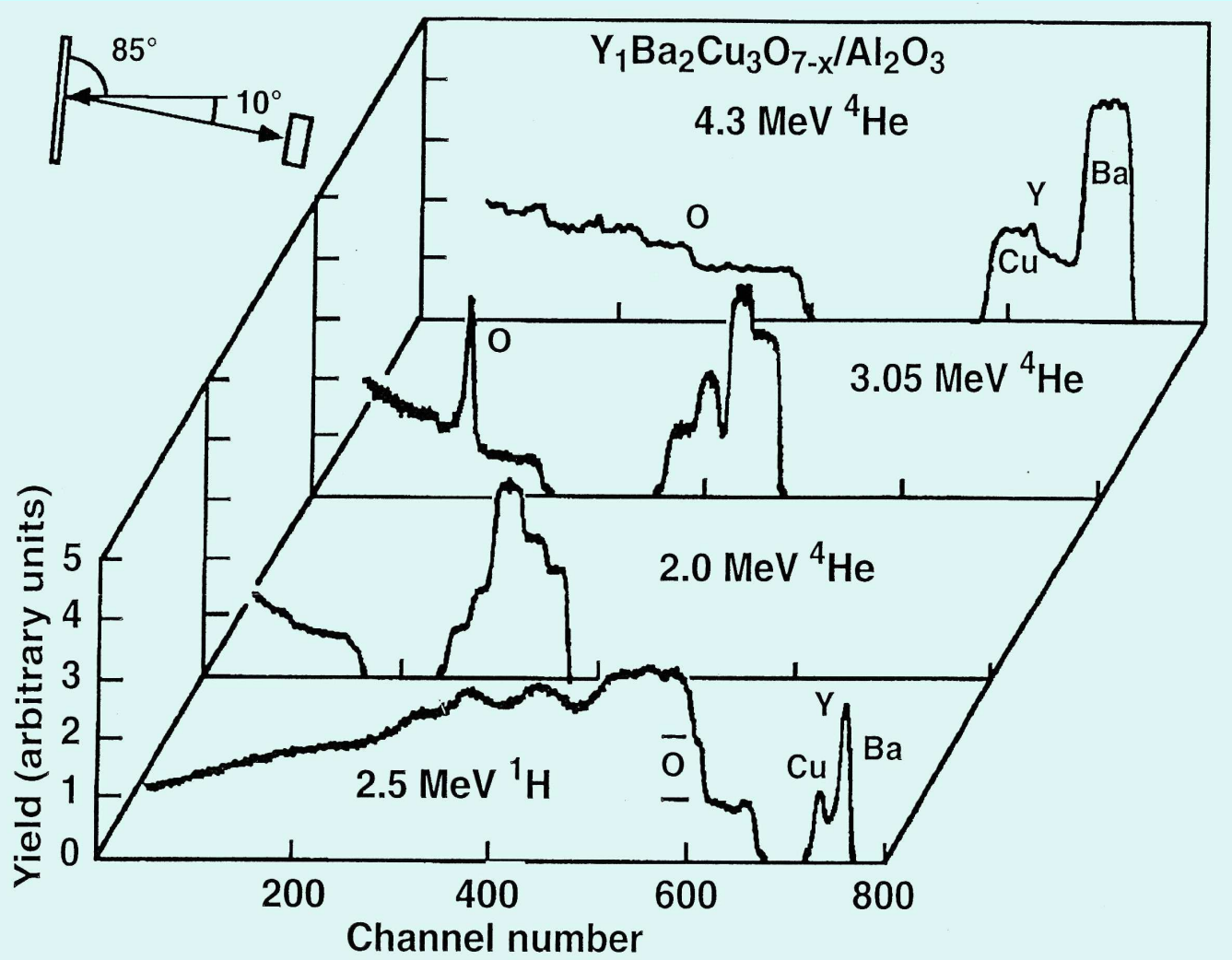

It is to be noted that the geometry of the sample does not fit the order of the peaks in the RBS spectrum

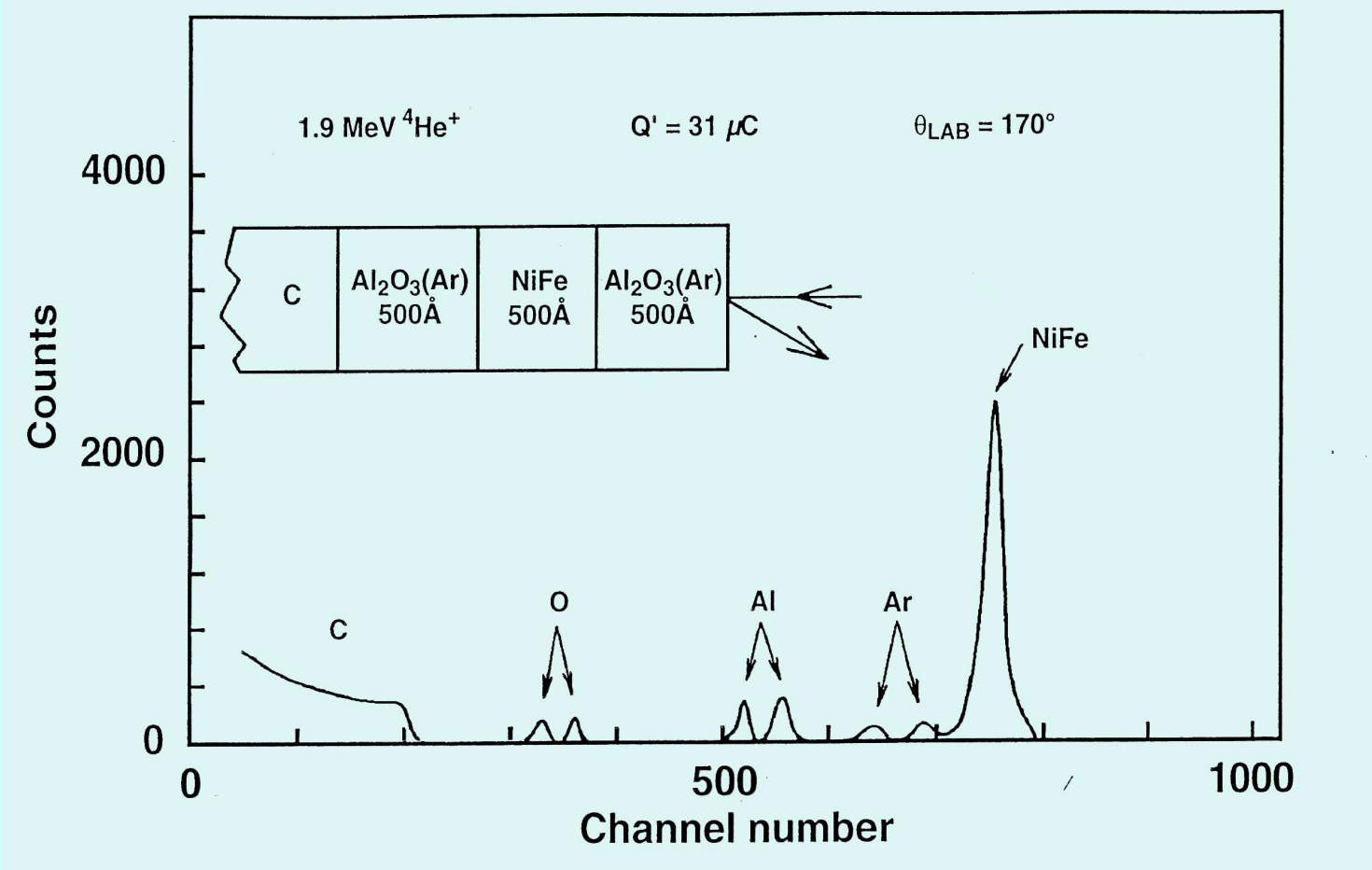

RBS spectra from metal layers on Al_2O_3 substrates

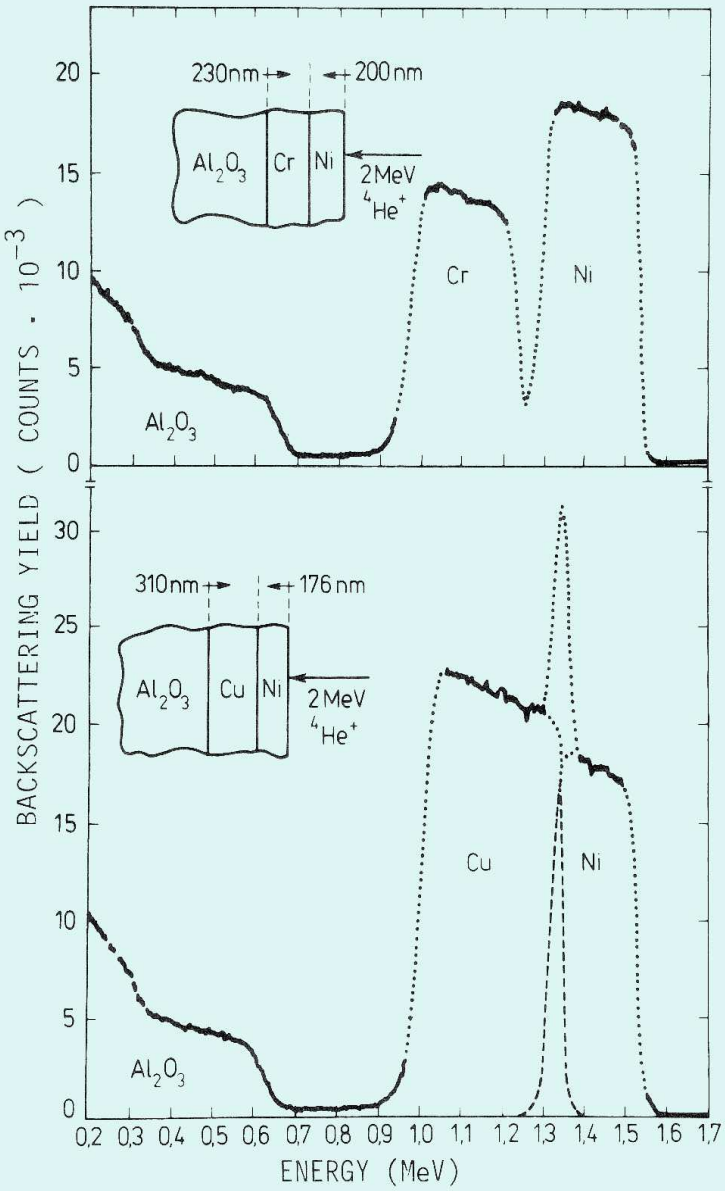

Distribution of recoil atoms by Monte-Carlo (TRIM) simulation for two GMR thin film systems

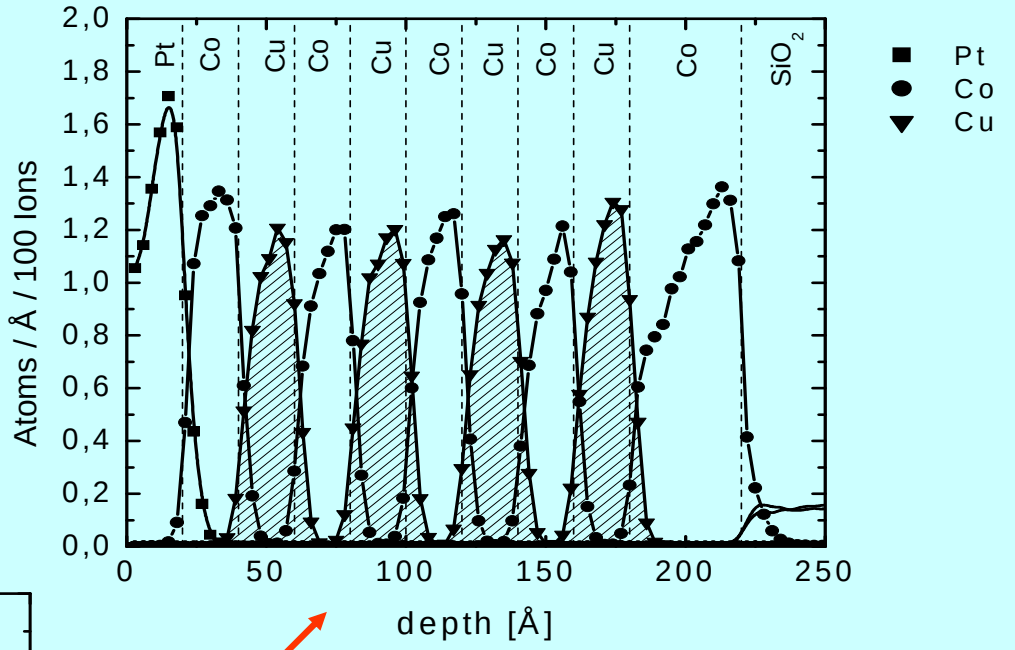

Pt(2nm)/[Co(2nm)/Cu(2nm)]$_4$/Co(4nm)/SiO$_2$

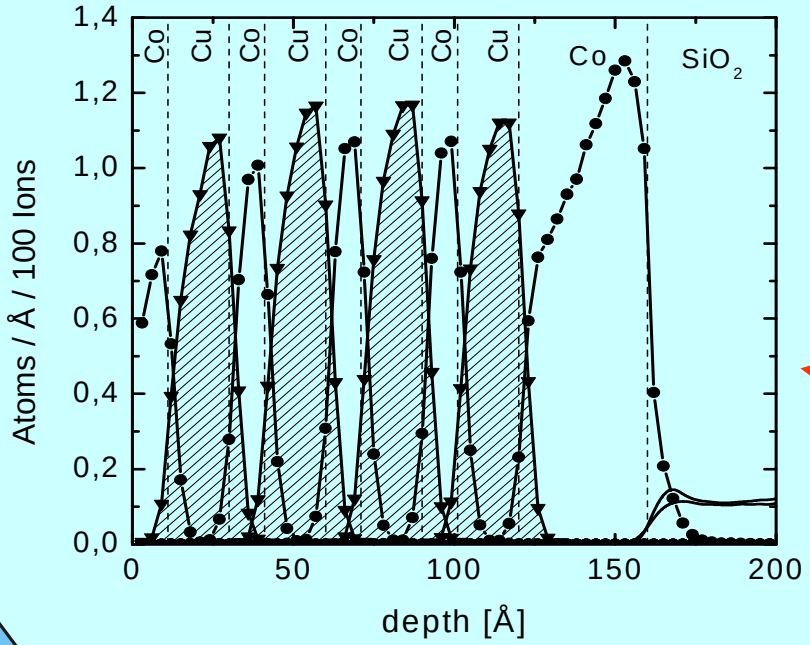

[Co(1.1nm)/Cu(1.9nm)]$_4$/Co(4nm)/SiO$_2$

RBS measurements with nanometer resolution: fitted concentration depth profiles. The Co/Cu layers are strongly intermixed

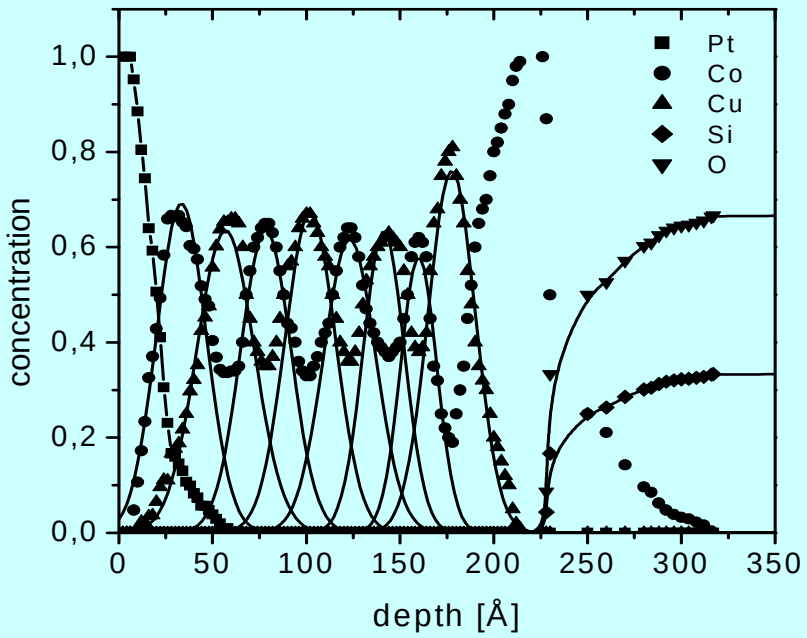

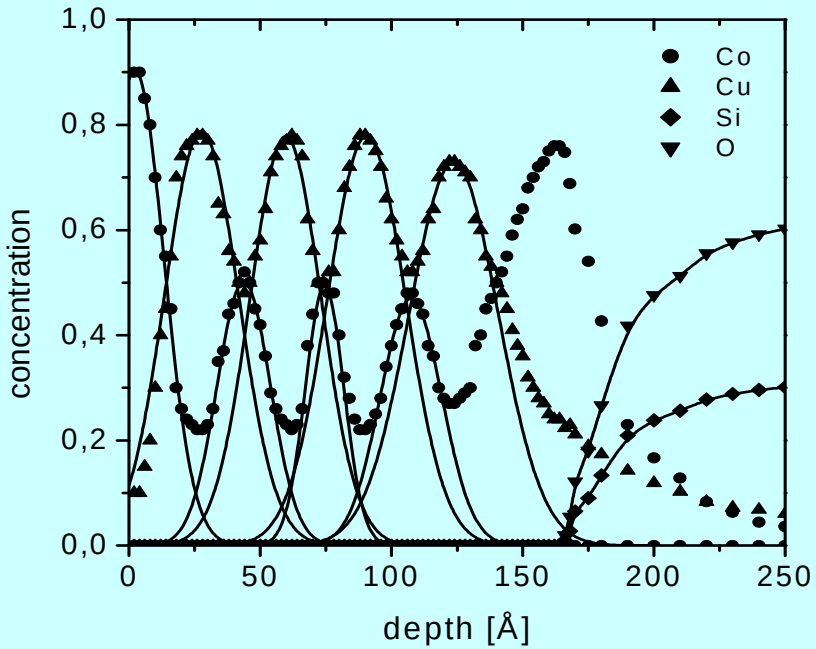

$[Co(1.1nm)/Cu(1.9nm)]_4/Co(4nm)/SiO_2$

$Pt(2nm)/[Co(2nm)/Cu(2nm)]_4/Co(4nm)/SiO_2$

RBS vs. NRA

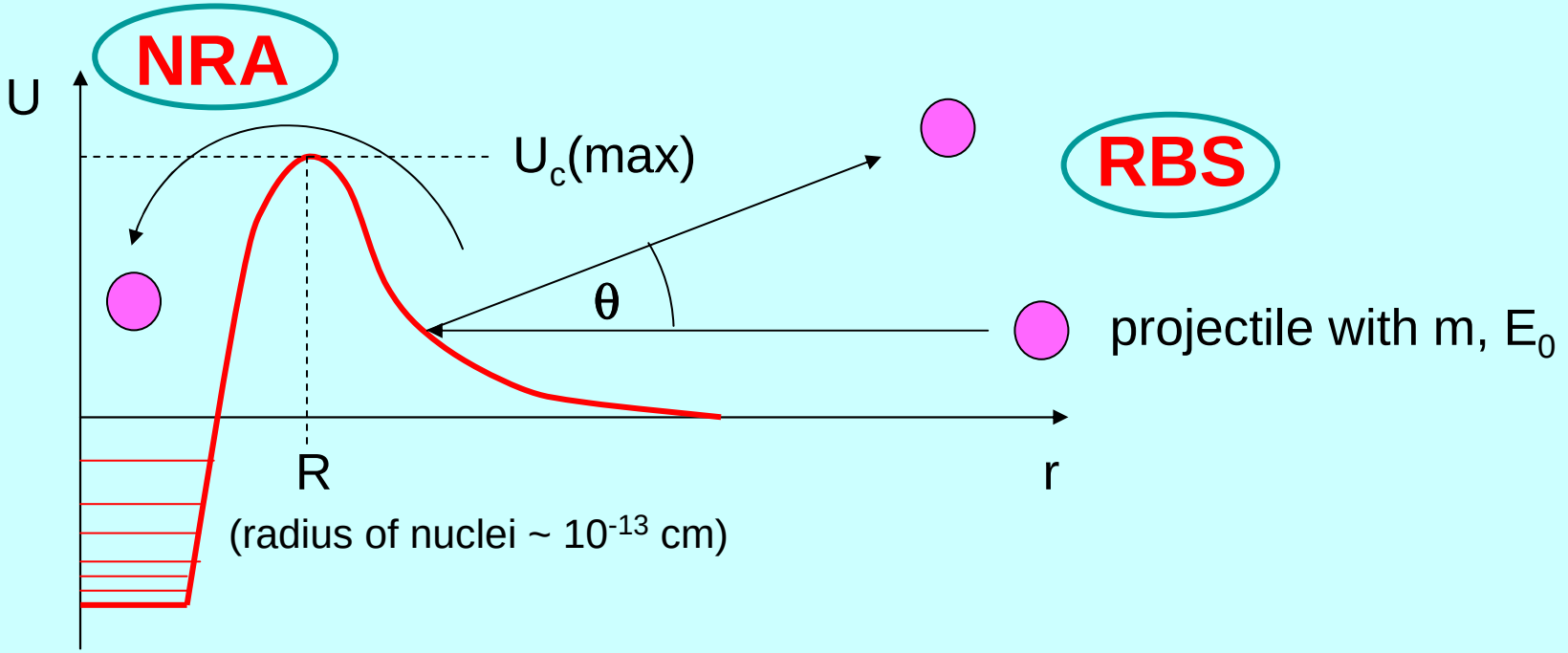

$$U_C(\max) = \frac{Z_1 Z_2 e^2}{R} \approx \frac{Z_1 Z_2 e^2}{A^{1/3}} [\mathrm{MeV}]$$

Channeling

Crystall lattice from Channeling (aligned) and RBS (random) view

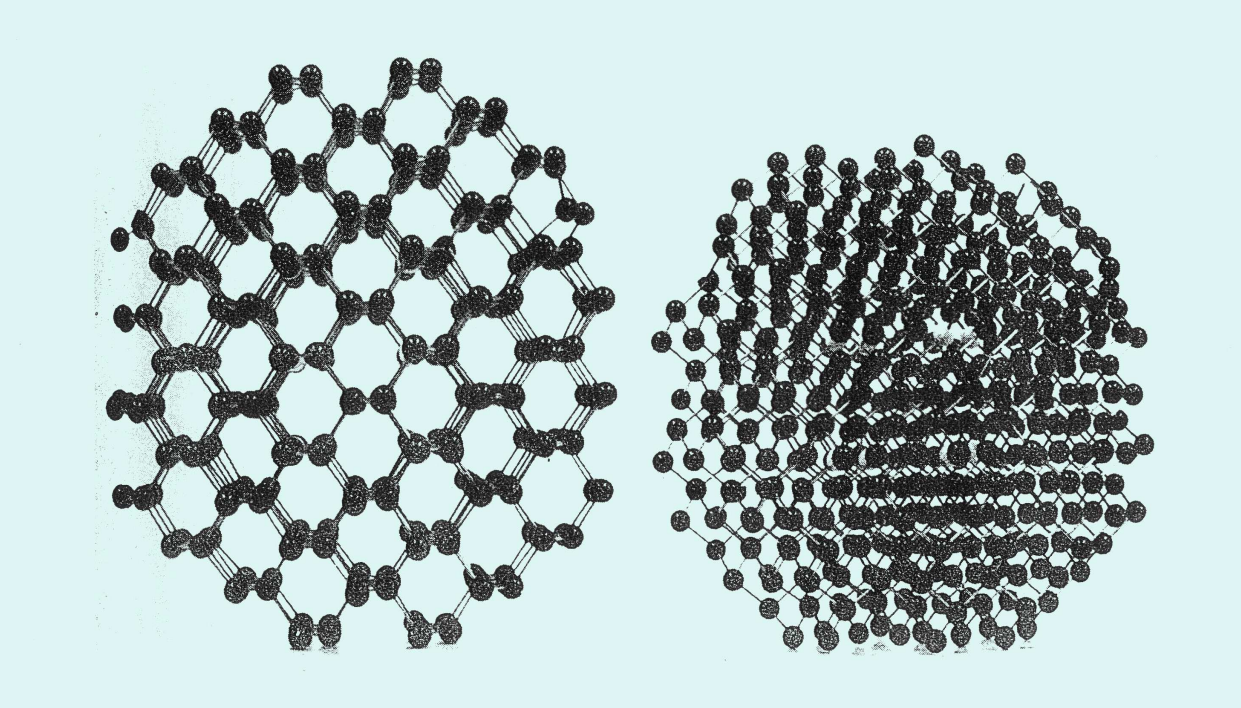

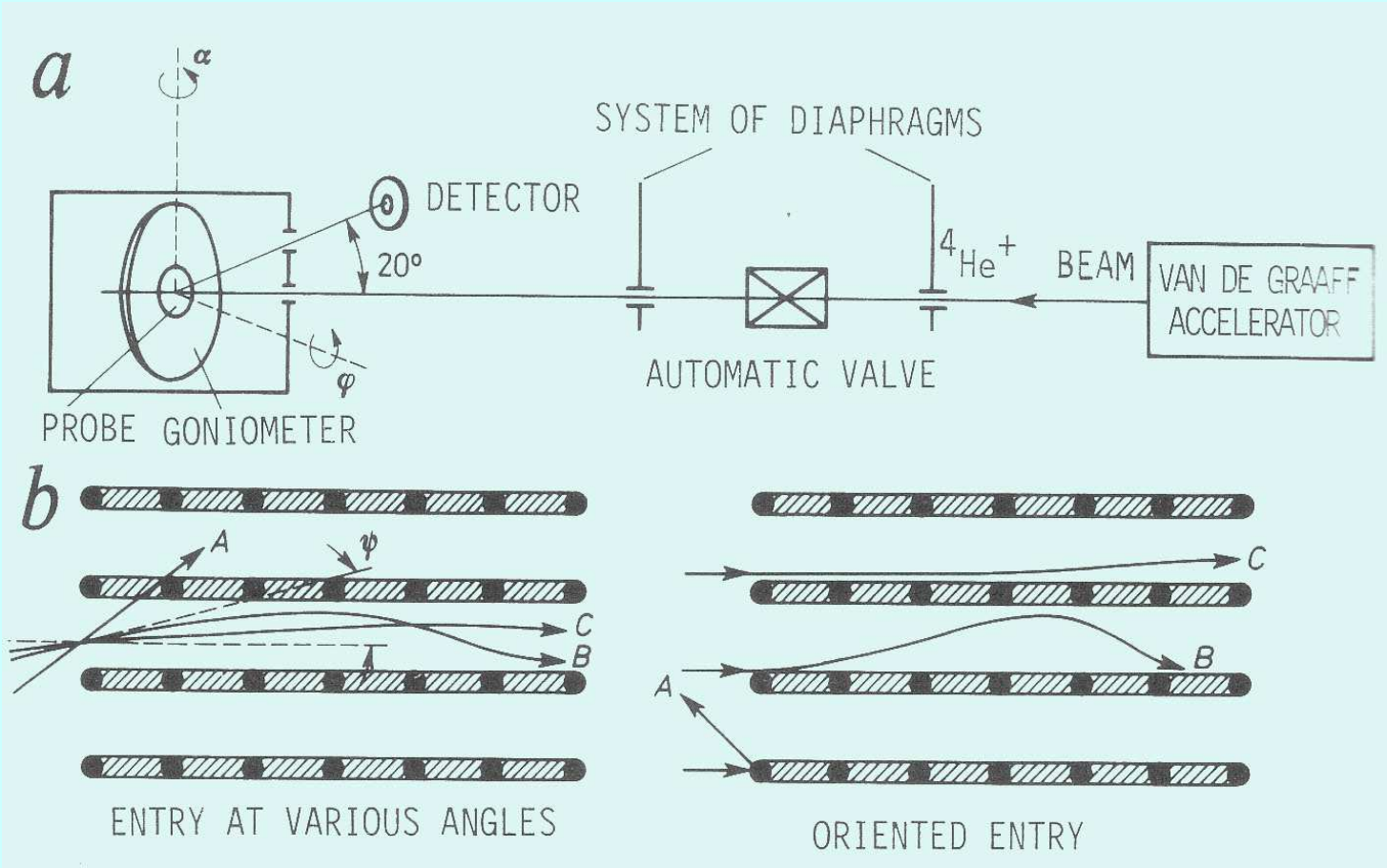

RBS measurements using the channeling effect:
(a) lay-out of the apparatus,
(b) principle of the channeling effect

Trace of an ion with angle φ in a lattice channel

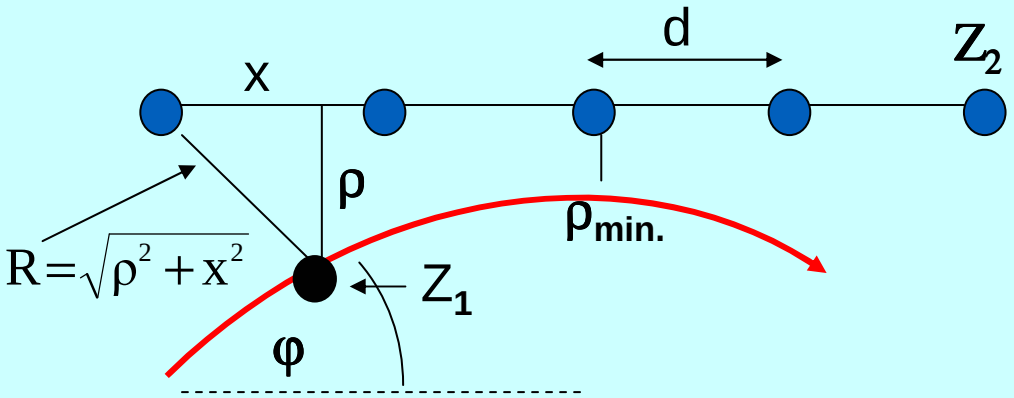

continuum modell of Lindhard:

atoms are equally charged;

the wall potential has the average value of the atomic potantials

According the theory of Lindhard is the potential:

$$U(\rho)=\frac{1}{d}\int V(R)dx$$

V(R) is the atomic potential (e.g. Thomas-Fermi potential)
The critical angle is:

$$\varphi_c=\left[U(\rho_{min})/E\right]^{\frac{1}{2}}$$

or as an approach:

$$\varphi_c=\left(2Z_1Z_2e^2/Ed\right)^{\frac{1}{2}}$$

for typical RBS measurements with 1-2 MeV He^+ ions it has the value of about 1°

Dependence of the channeling spectrum on the angle

I(RBS) / I(aligned)

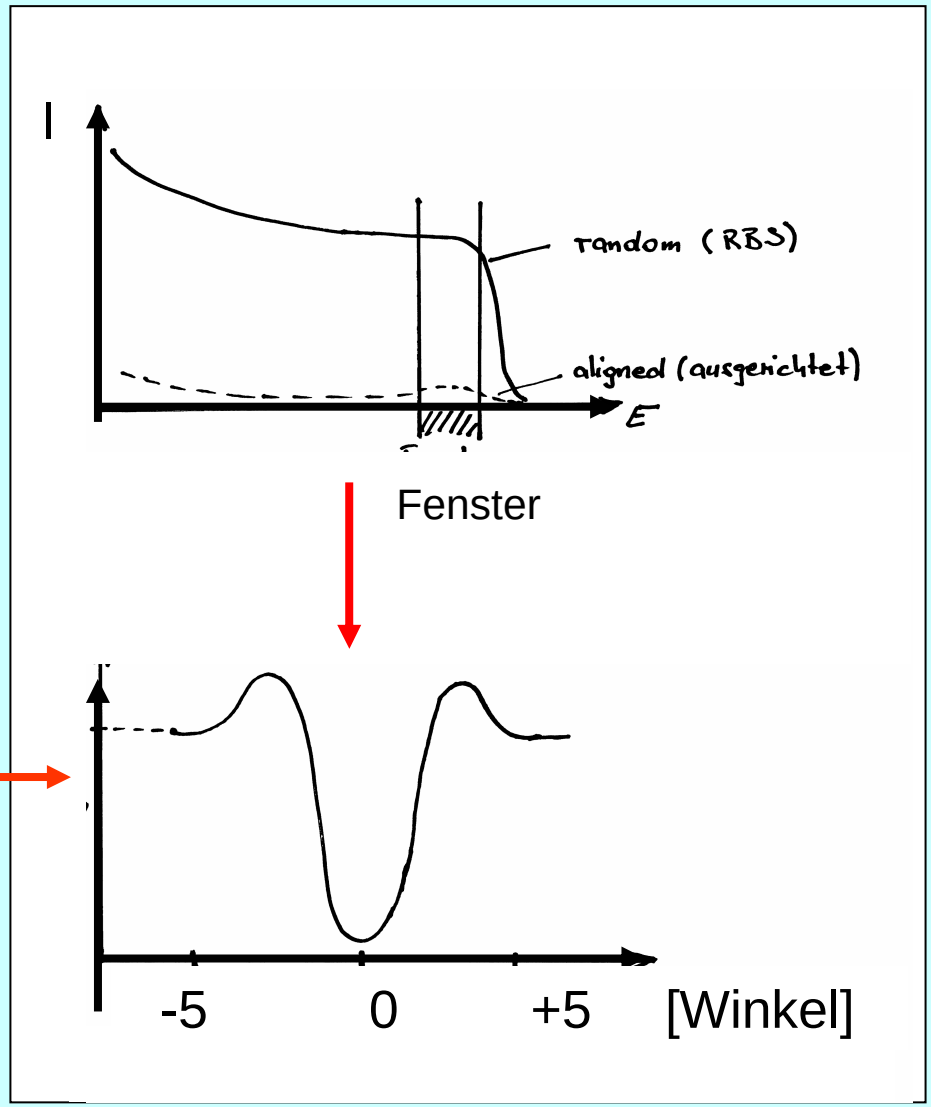

Channeling differential curves

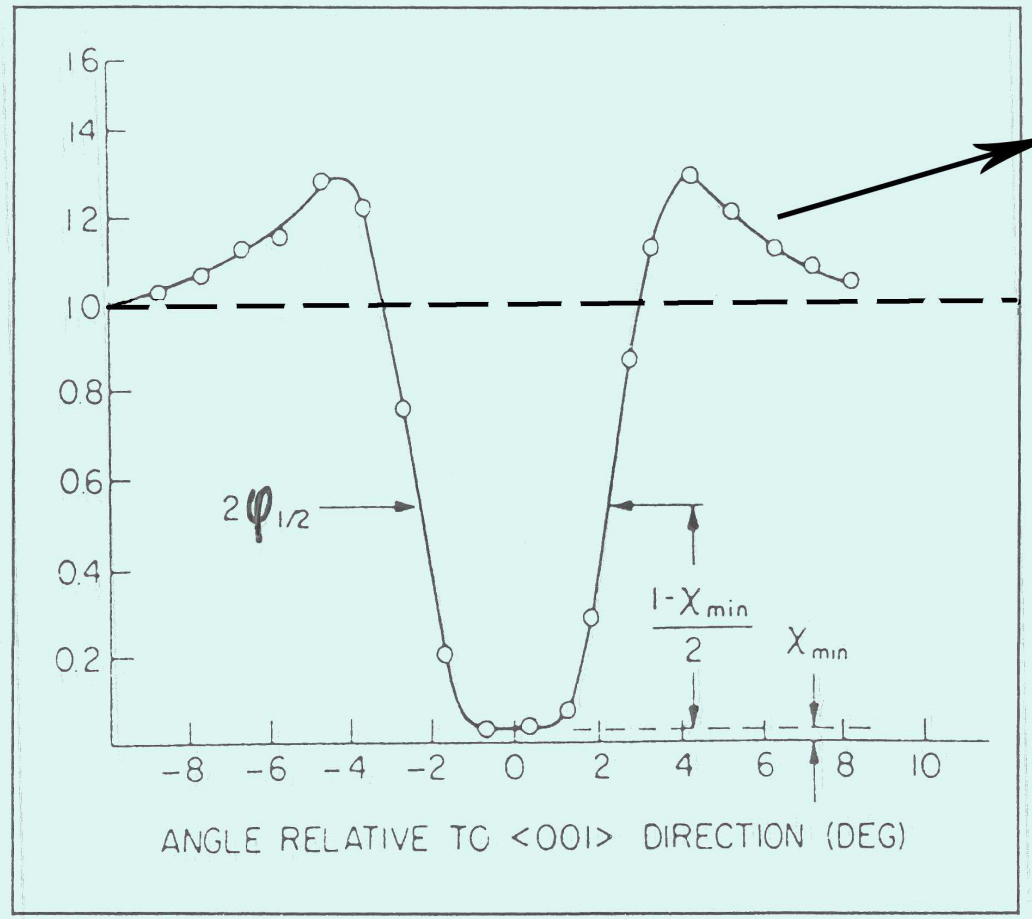

Channeling curves of magnetite/MgO epitaxially grown layers.

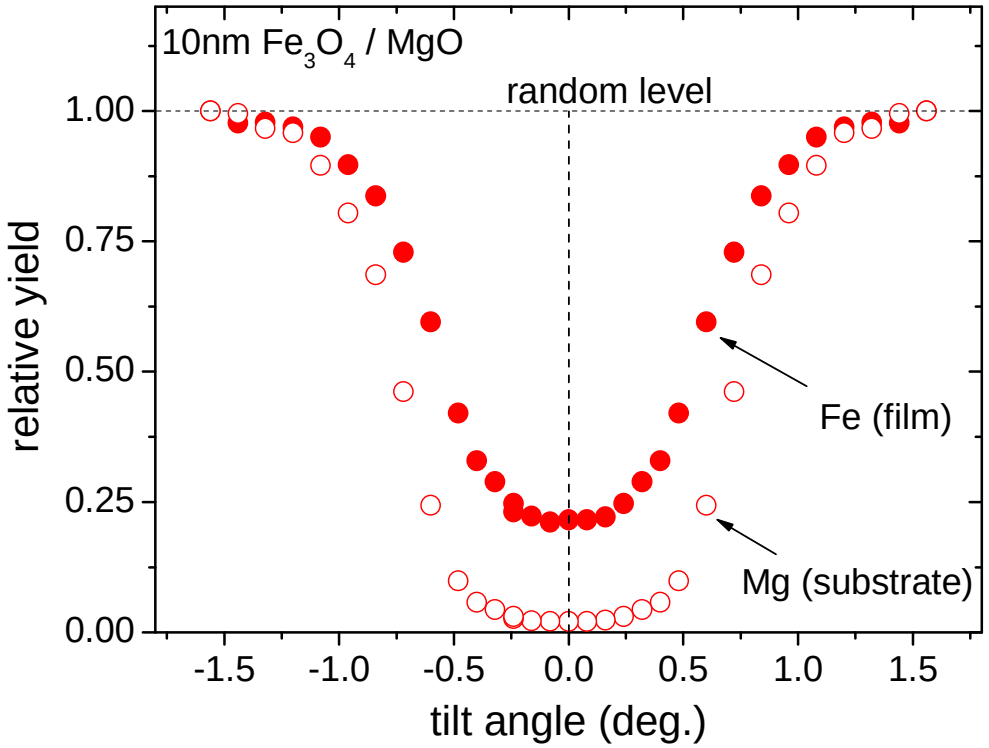

Random and aligned spectra of an a-Si/c-Si sample

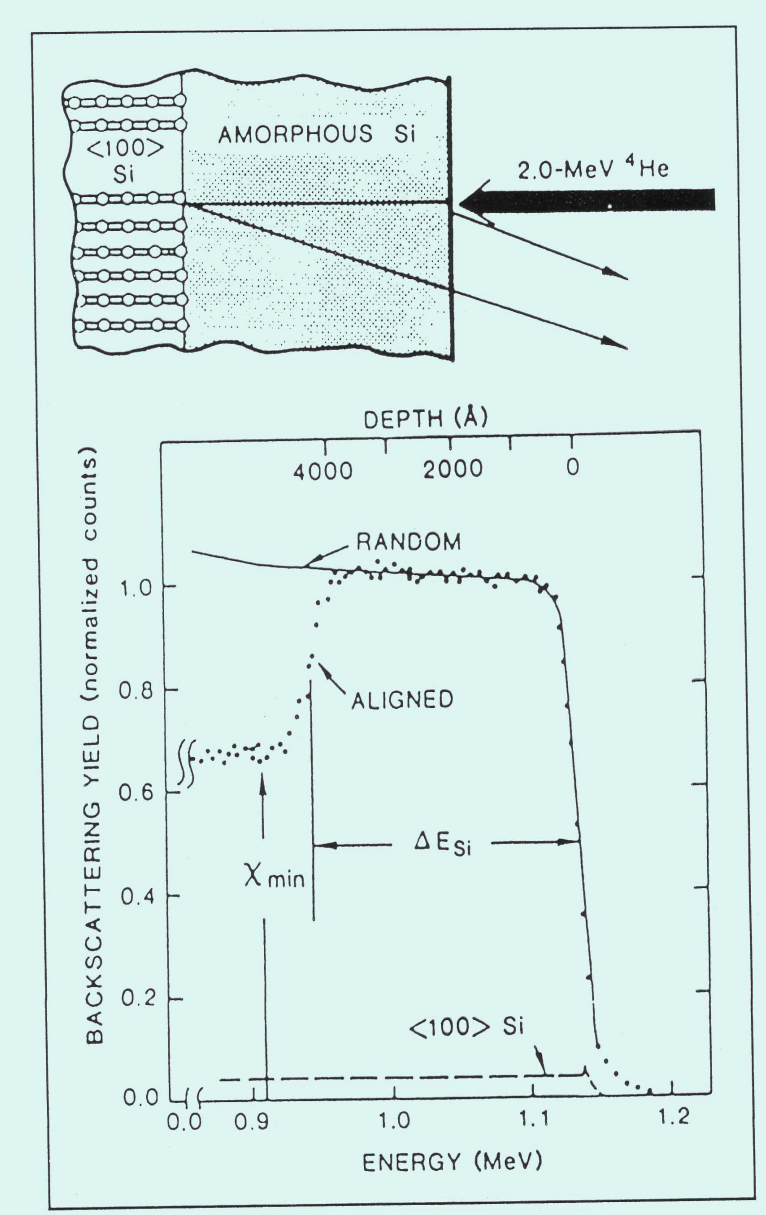

Implantation into Si

The implanted As is on a substitutional lattice place

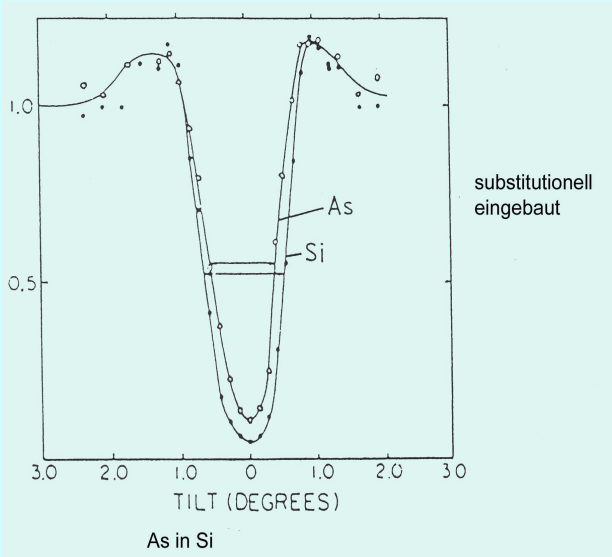

substitutionell eingebaut

As in Si

The implanted Yb is on an interstitial lattice place („flux peaking effect“ at the centre of a channel)

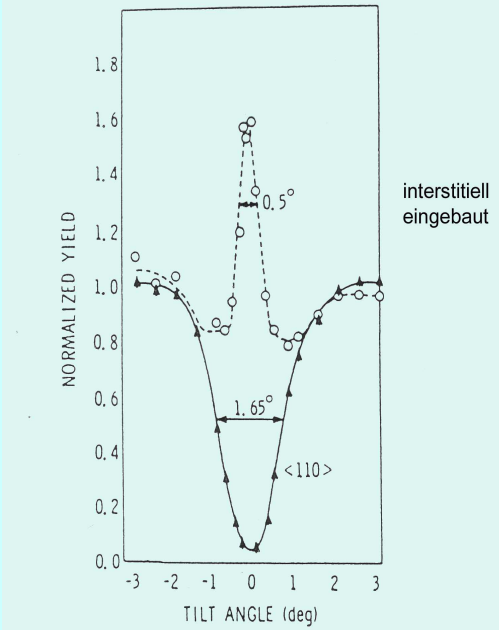

interstitiell eingebaut

RBS spectrum of a burried $CoSi_2$-layer

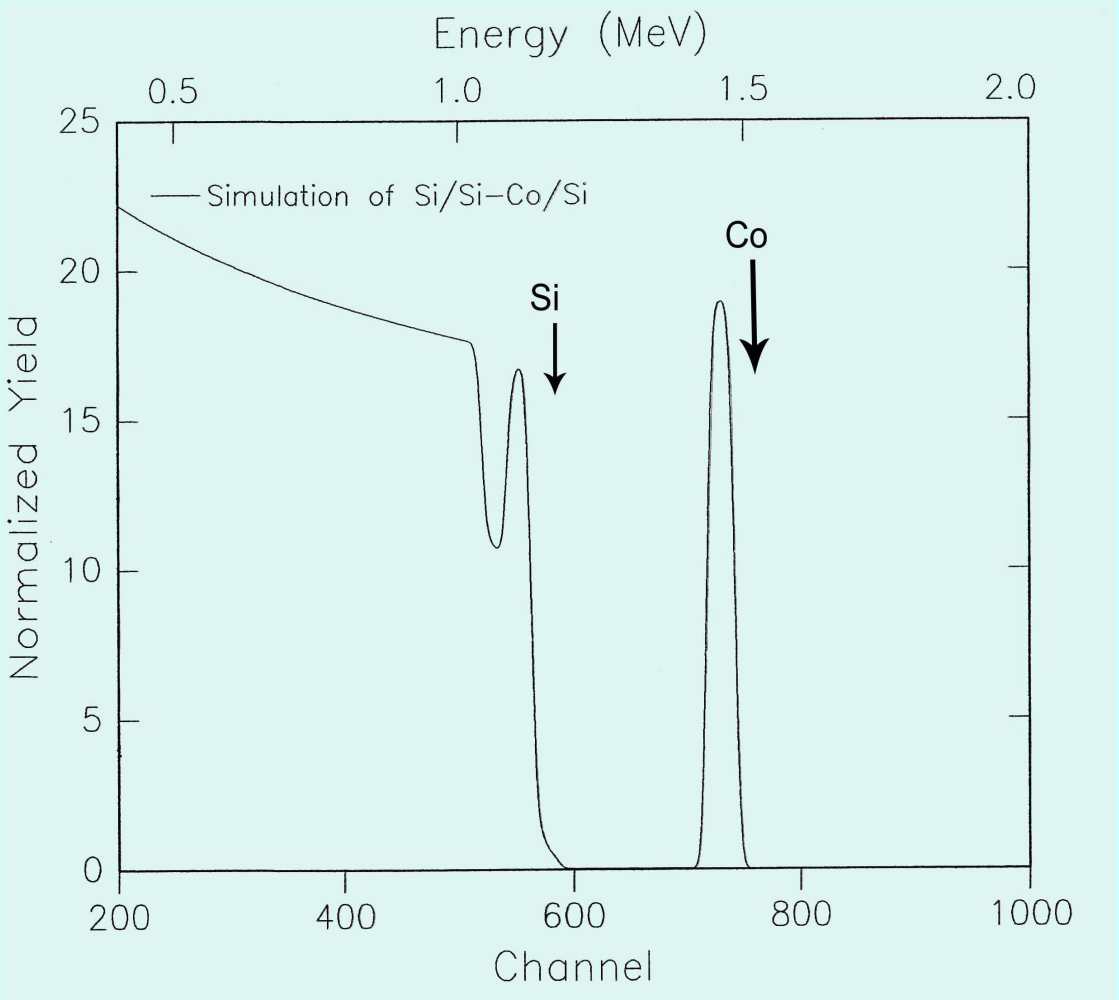

3D-spectrum of the burried silicide layer

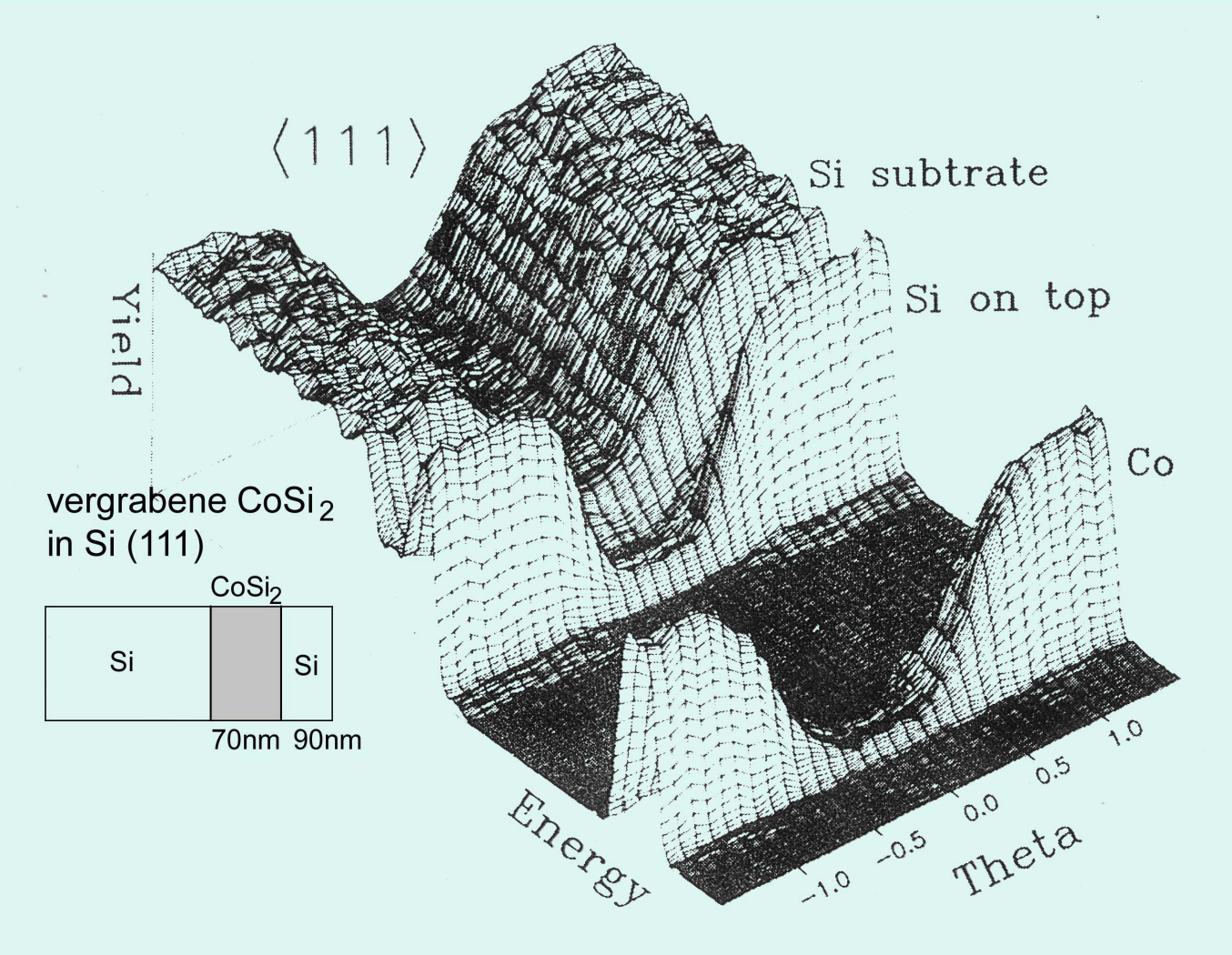

Channeling set-up in the Institut für Kernphysik, Uni Frankfurt

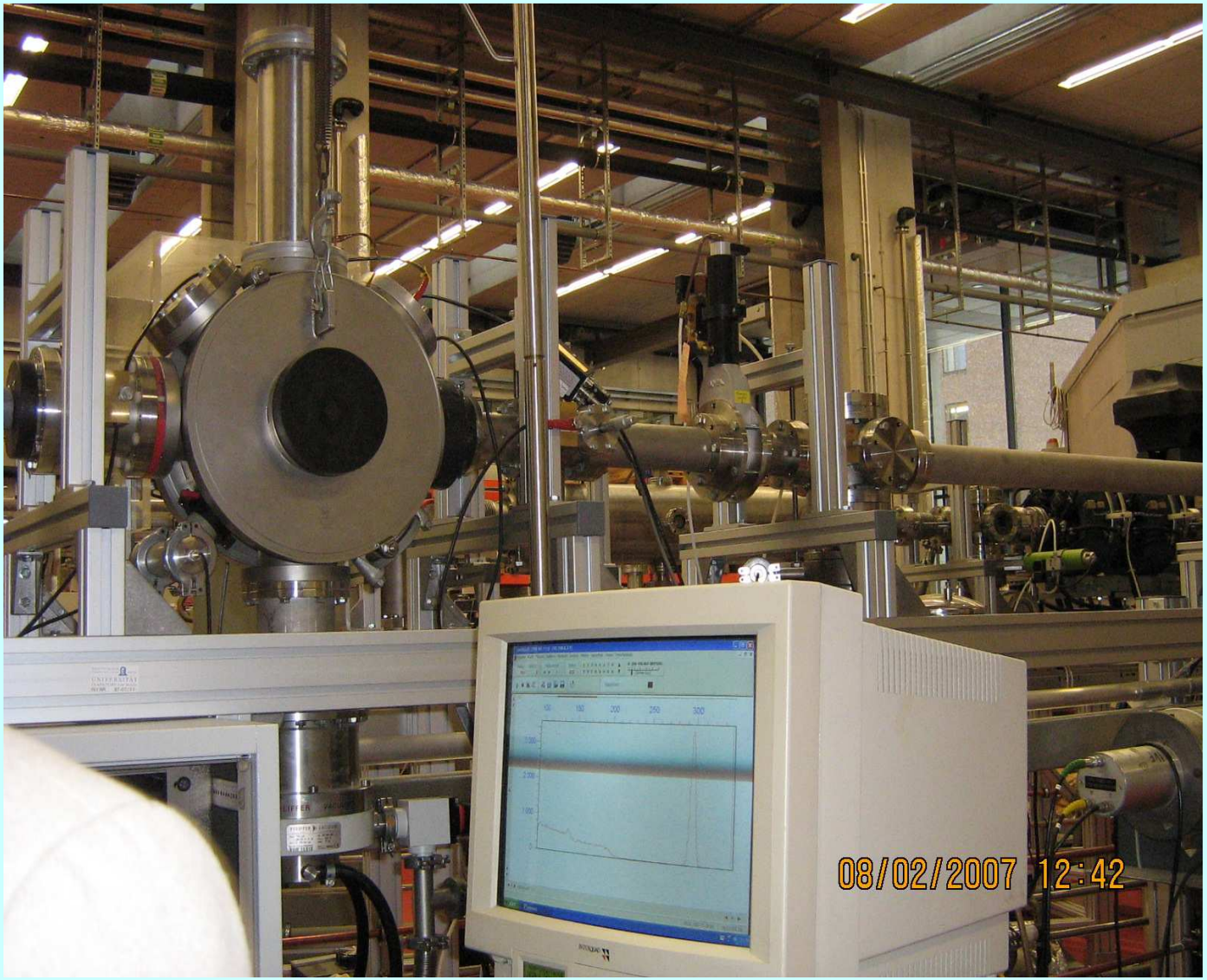

Stepping Motor and Goniometer

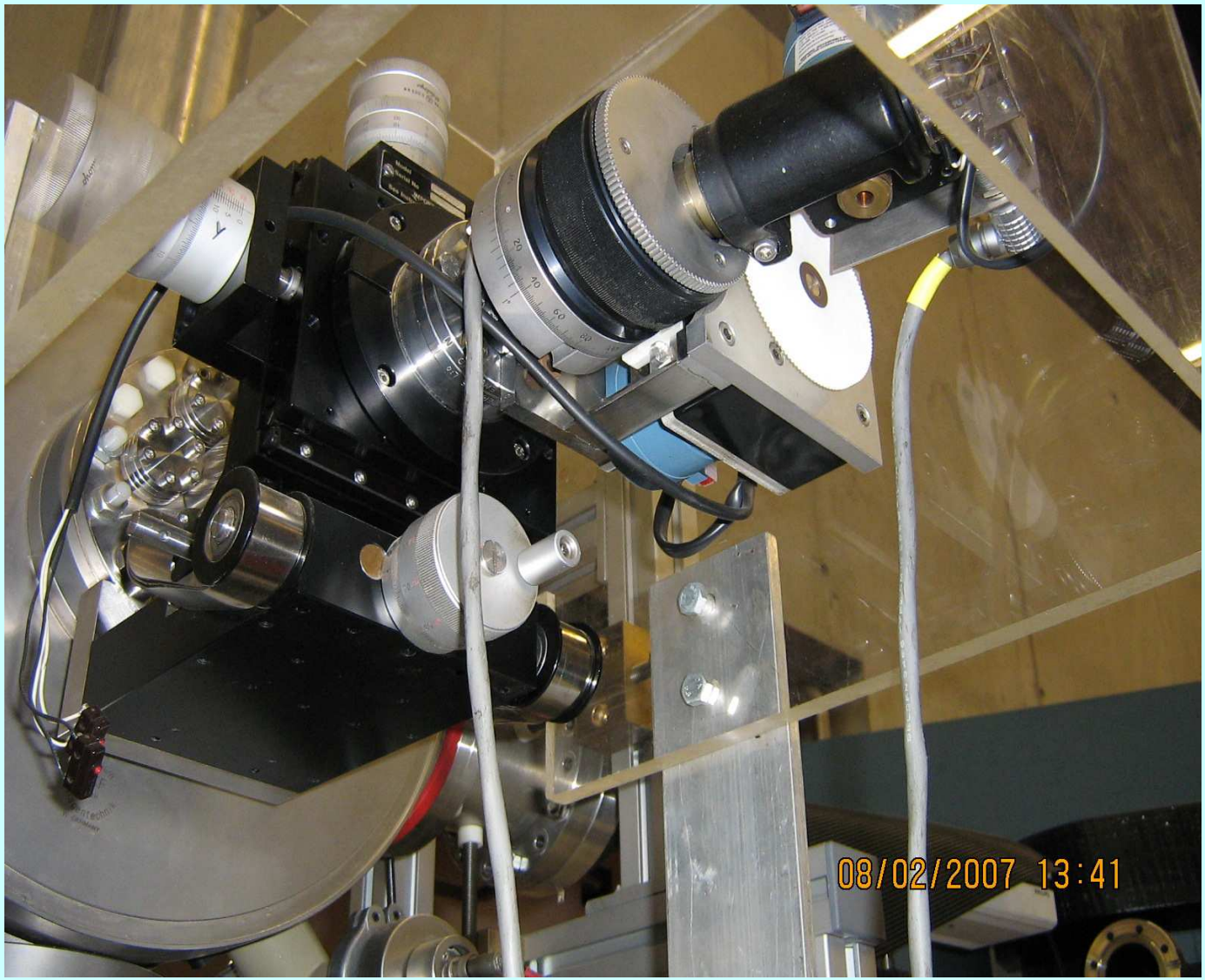

Scattering chamber with detector

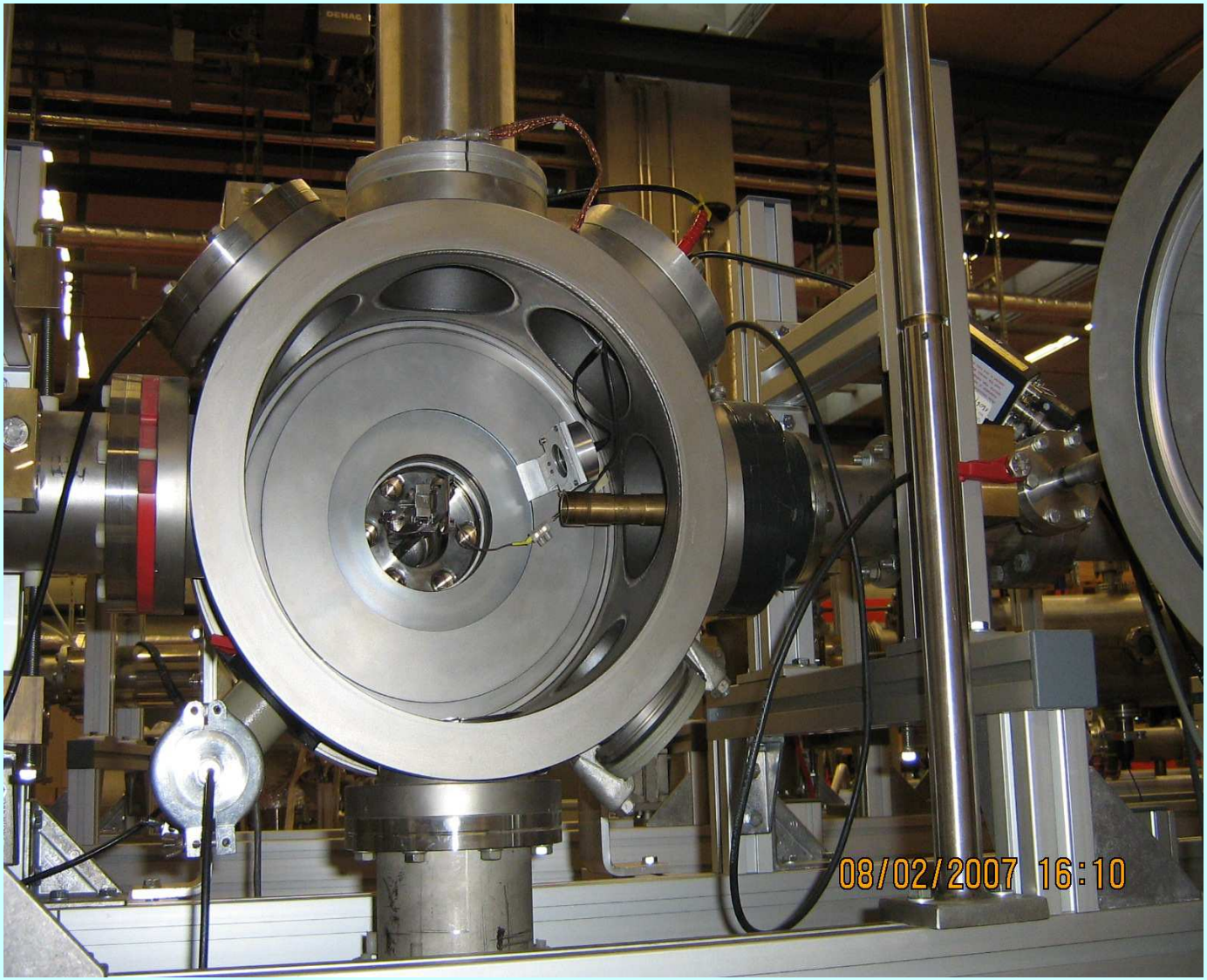

Nuclear Reaction Analysis (NRA)

First nuclear reactions that have been performed:

Rutherford, 1919 $\alpha + {}^{14}\mathrm{N} \rightarrow {}^{17}\mathrm{O} + \mathrm{p}$

$${}^{14}\mathrm{N}(\alpha,\mathrm{p}){}^{17}\mathrm{O}$$

Cockroft-Walton, in 1932 using 1 MeV protons

$$\mathrm{p} + {}^{7}\mathrm{Li} \rightarrow 2\alpha$$

Conservation laws that have to be considered:

-energy
-momentum
-moment of momentum
-charge
-atomic number
-parity

Two kind of nuclear reactions:
resonant and not-resonant

I. resonant nuclear rections (requested):
reaction cross section changes strongly with energy (E_R)

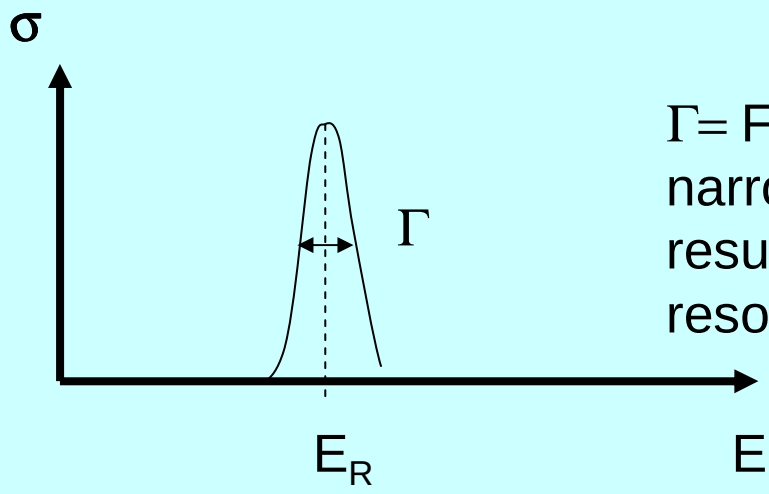

Γ= FWHM of the reaction
narrow Γ (< 100 eV)
results in good depth
resolution

II. not-resonant nuclear reaction:
cross section changes smoothly with energy

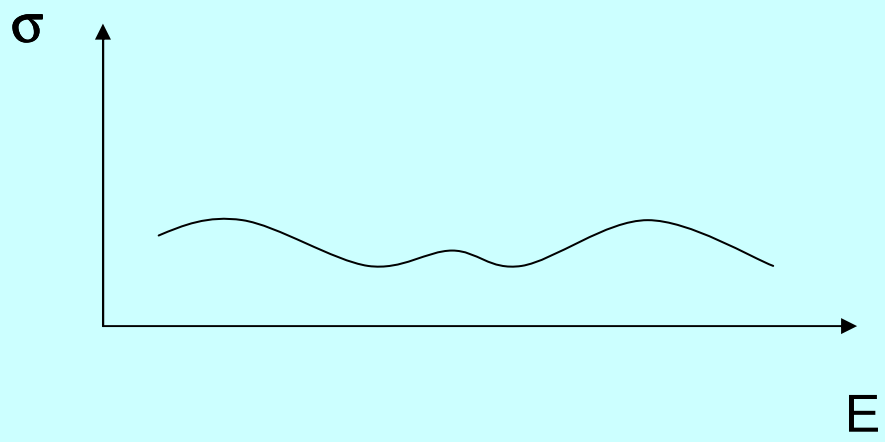

Dependence of cross section on energy for protons and α– particles in different targets

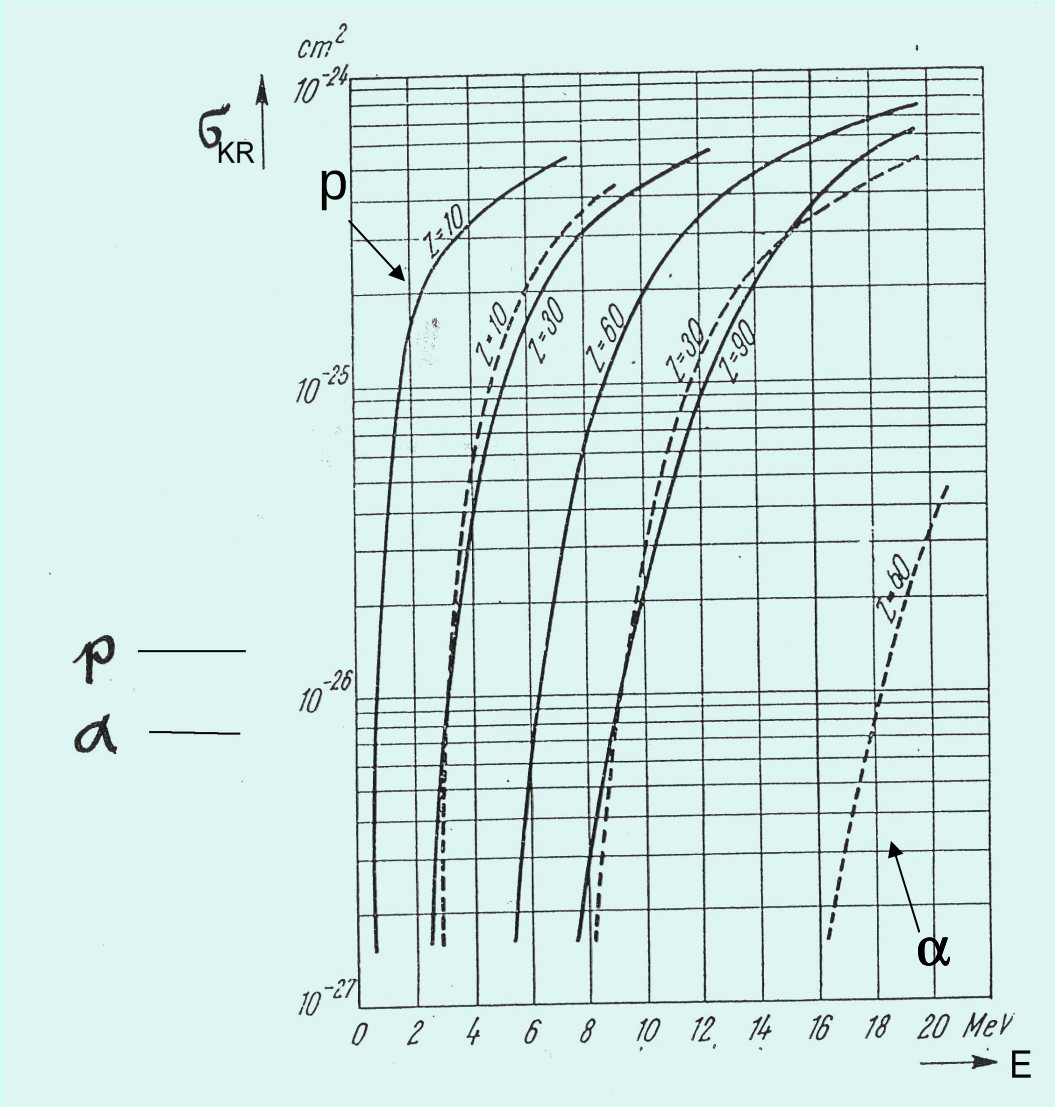

some (p,γ) and (p,γα) reactions in low energy range between 473 and 675 keV.

special importance has the (p,γ)- reaction for Al profiling with a FWHM of <60 eV.

Proton Energy (kev)	Reaction	Gamma-Ray Energy (Mev)	Cross Section (mb)	Width (kev)	References (author and year)
473	$Mg^{25}(p,\gamma)Al^{26}$				Br 56a
484	$F^{19}(p,\alpha\gamma)O^{16}$	7.12, 6.92, 6.13	>32	0.9	Bo 58, Bu 56, Ch 50
496	$Mg^{25}(p,\gamma)Al^{26}$	6.36, 4.24, 4.21 ?		5	Hu 55, Hu 54, Kl 54
500	$Si^{30}(p,\gamma)P^{31}$	7.75, 6.48, 4.62			Br 58, Br 56a
504	$Al^{27}(p,\gamma)Si28$	12.07		<0.20	An 58
506	$Al^{27}(p,\gamma)Si^{28}$	10.29		<0.17	An 58
511	$Na^{23}(p,\gamma)Mg^{24}$	10.8, 8.0, 6.9		0.8	Ba 56, Gr 55, Ha 55
513	$Mg^{25}(p,\gamma)Al^{26}$			3	Hu 55, Hu 54, Kl 54
530	$Mg^{25}(p,\gamma)Al^{26}$			3	Hu 55, Hu 54, Kl 54
532	$C^{14}(p,\gamma)N^{15}$	10.7, 5.3			He 58, Ba 55
540	$P^{31}(p,\gamma)S^{32}$				Ke 56, Gr 51, Ta 46
550	$C^{13}(p,\gamma)N^{14}$	8.06, 4.11	1.44	32.5	Br 57, Wo 53, Se 52
580	$Mg^{25}(p,\gamma)Al^{26}$	6.85 ?, 6.43, 4.28			Kl 54, Ta 54
594	$Na^{23}(p,\gamma)Mg^{24}$	10.9, 8.0, 7.0		2	Ba 56, Pr 56, Gr 55
594	$S^{32}(p,\gamma)Cl^{33}$	2.86, 2.05, 0.806			Va 56a
597	$F^{19}(p,\alpha\gamma)O^{16}$	7.12, 6.92, 6.13	7.1	30	Hu 55a, Ch 50, Bo 48
607	$Mg^{25}(p,\gamma)Al^{26}$	6.88 ?, 6.46, 4.34			Kl 54, Ta 54
612	$Al^{27}(p,\gamma)Si^{28}$			<1	An 58, Br 47, Ta 46
625	$Si^{30}(p,\gamma)P^{31}$	7.87			Br 58, Br 56a, Ts 56
630	$O^{18}(p,\gamma)F^{19}$	8.5		2.6	Bu 55
632	$Al^{27}(p,\gamma)Si^{28}$	10.41, 7.59, 1.77		<0.06	An 58, Ru 54, Br 47
636	$Ne^{22}(p,\gamma)Na^{23}$	9.40			Th 58, Br 47a
640	$C^{14}(p,\gamma)N^{15}$	10.8, 5.3			He 58, Ba 55
648	$P^{31}(p,\gamma)S^{32}$			17	Ke 56, Fr 51, Gr 51
650	$Ca^{40}(p,\gamma)Sc^{41}$				Bu 58
654	$Al^{27}(p,\gamma)Si^{28}$	10.43, 7.61		<0.06	An 58, Br 47, Ta 46
660 ?	$Ne^{22}(p,\gamma)Na^{23}$				Th 58, Br 47a
661	$Mg^{26}(p,\gamma)Al^{27}$	7.88, 6.68, 5.9			Va 56b, Ru 54a
667	$Mg^{25}(p,\gamma)Al^{26}$				Kl 54, Ta 54
672	$F^{19}(p,\gamma)Ne^{20}$	11.88, 1.63	0.5	6.0	Fa 55, Hu 55, Si 54
672	$F^{19}(p,\alpha\gamma)O^{16}$	7.12, 6.92, 6.13	57	6.0	Hu 55a, Ch 50, Bo 48
675	$B^{11}(p,\gamma)C^{12}$	12.15, 4.43	0.050	322	Hu 53
675	$Na^{23}(p,\gamma)Mg^{24}$	11.0, 8.1, 7.1		≤1	Ba 56, Pr 56, Fl 54
675	$Mg^{25}(p,\gamma)Al^{26}$	6.55, 5.21, 3.30			Gr 56, Ka 55, Kl 54
675	$Si^{30}(p,\gamma)P^{31}$	7.92, 6.65, 1.27			Br 58, Br 56a

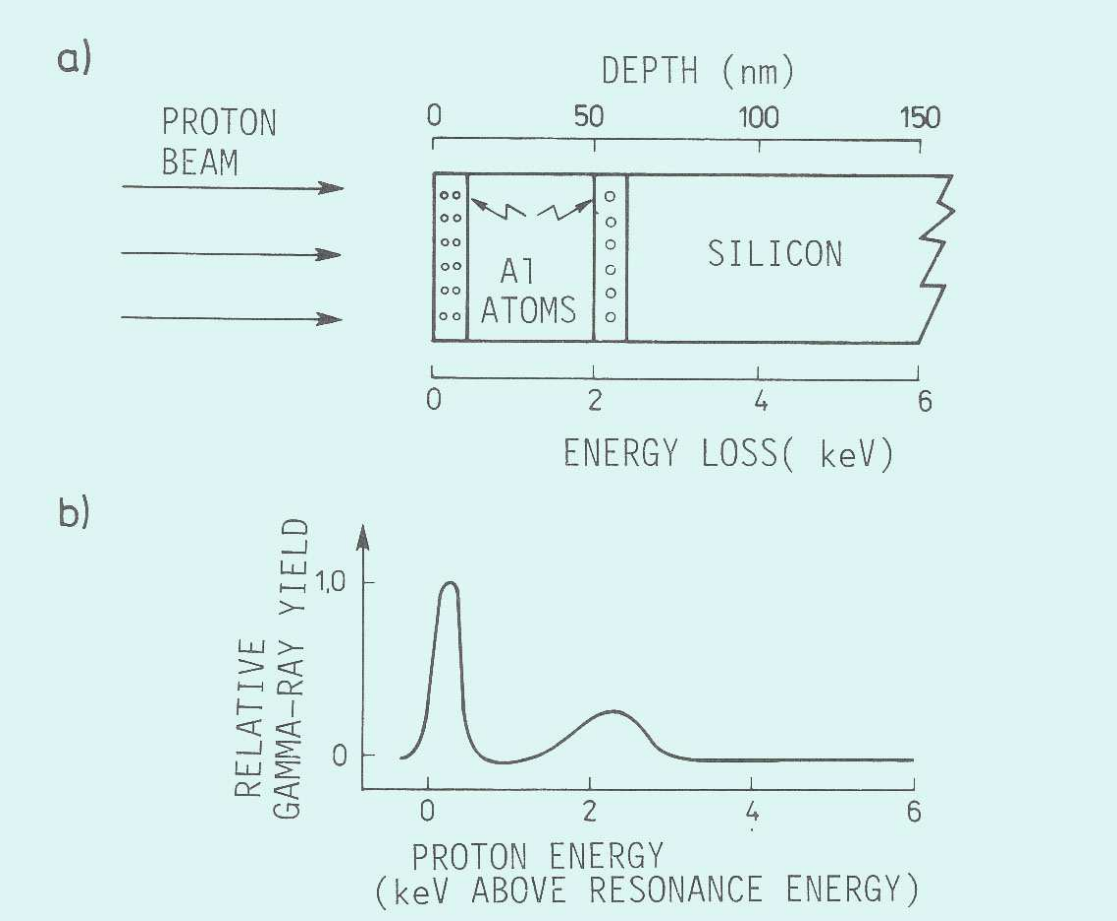

Resonance profiling of Al concentration in Si: (a) schematic diagram of the sample, (b) gamma-ray profiles as a function of proton enegy

N-15 method

H-profiling using the $^{1}H(^{15}N,\alpha\gamma)^{12}C$ reaction

Determination of concentration and depth profile of H

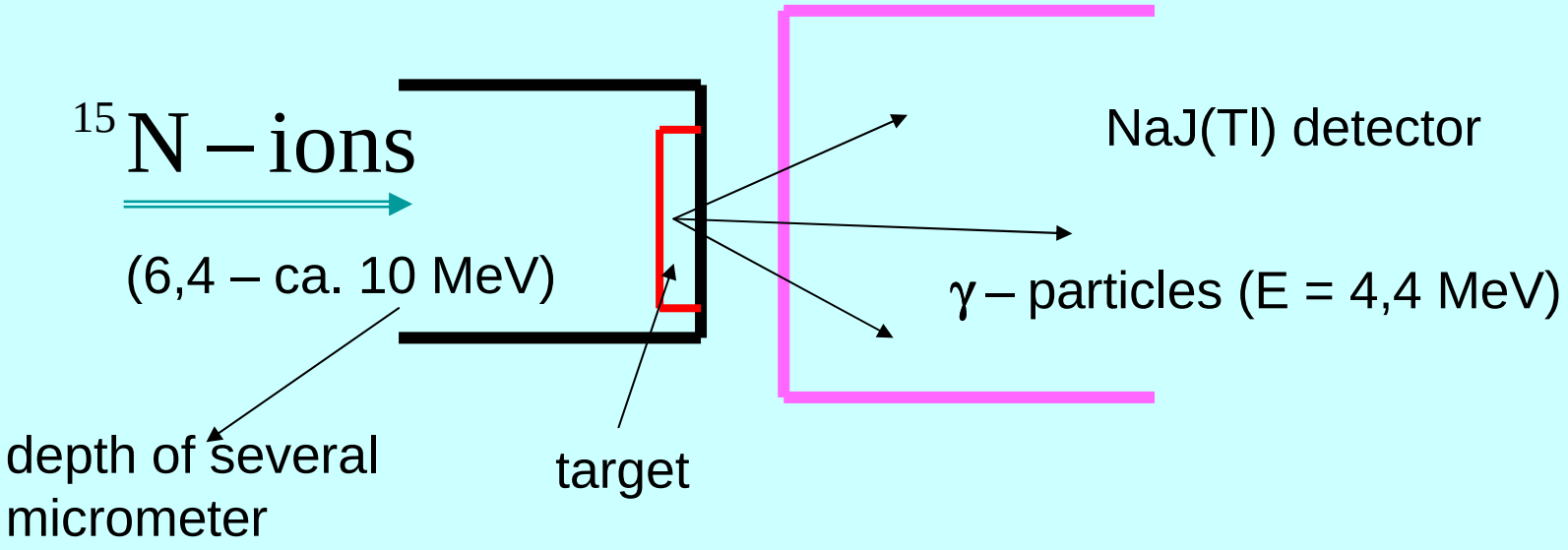

sensitivity of sintered Y-Ba-Cu-O high-T_c superconductors for humidity and H charging

H-Tiefenprofile zur Bestimmung der H-Konzentration (N-15 Methode)

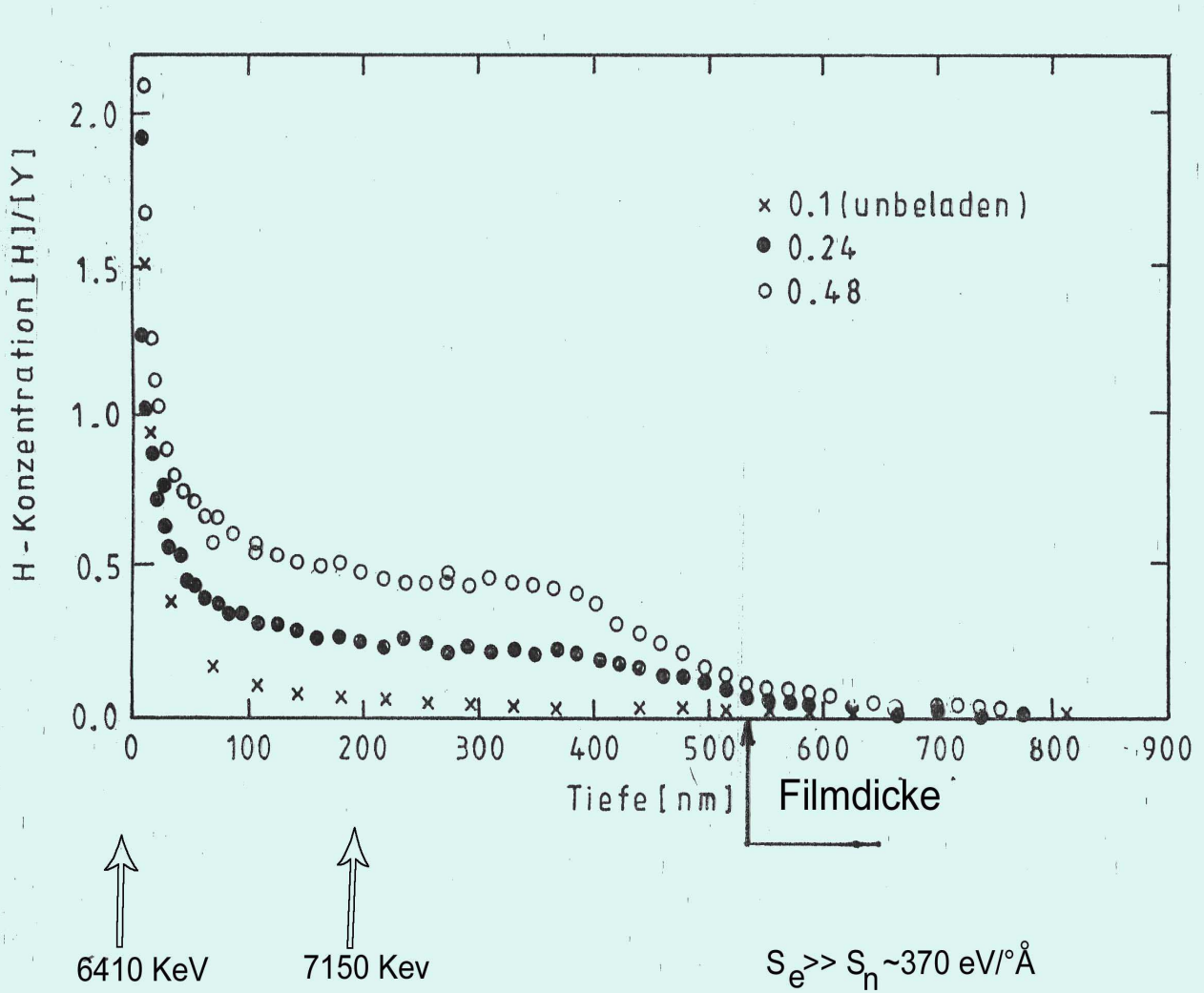

Secondary Ion Mass Spectrometry (SIMS)

The principle

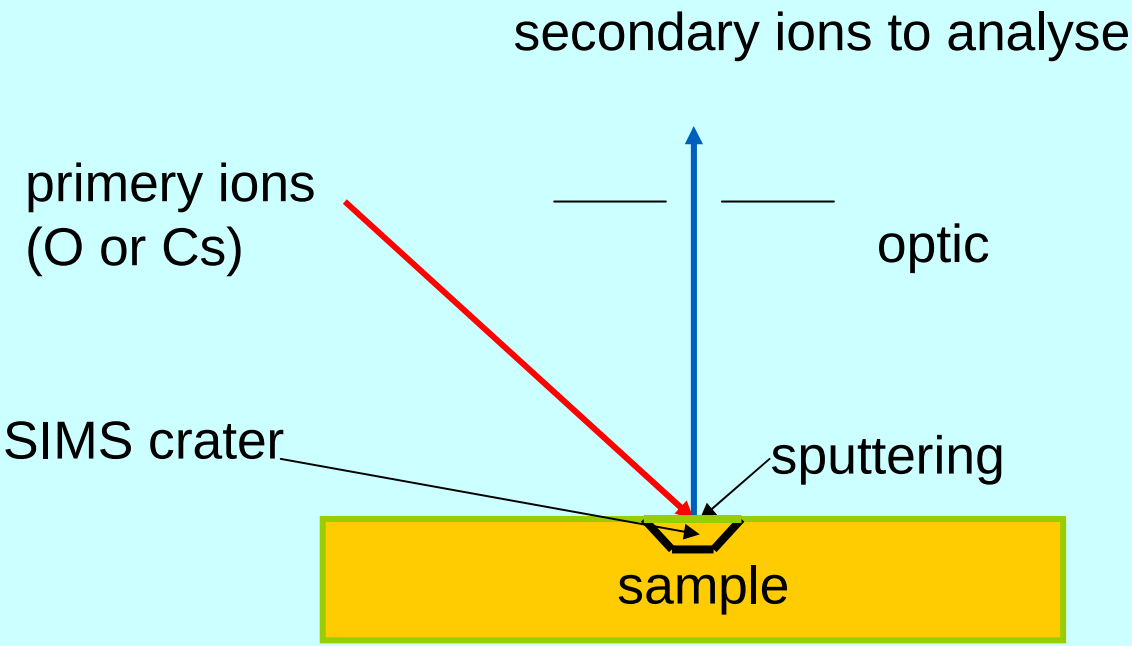

primery ions sputter the surface

↓

formation of SIMS crater and depth profile

↓

transformation of sputtering time into depth (frequently difficult)

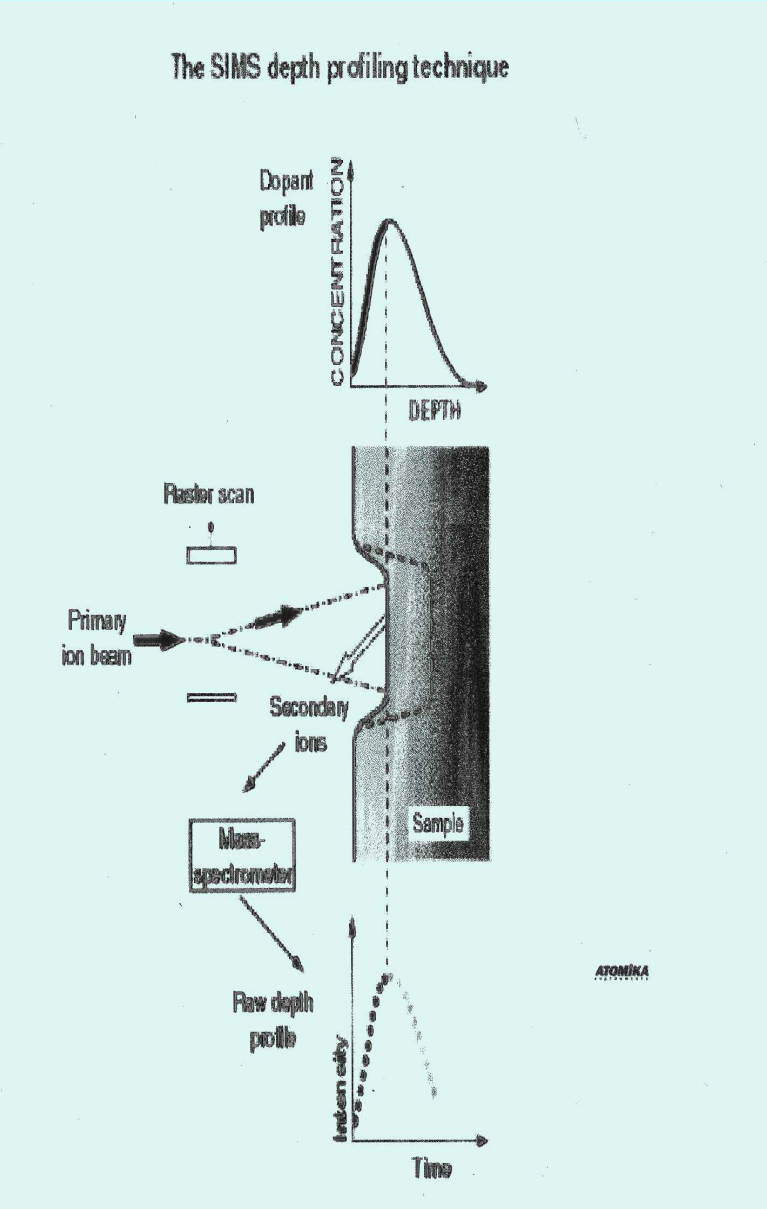

schematic set-up of the SIMS equipment at the Institute of Materials Science of the TUD

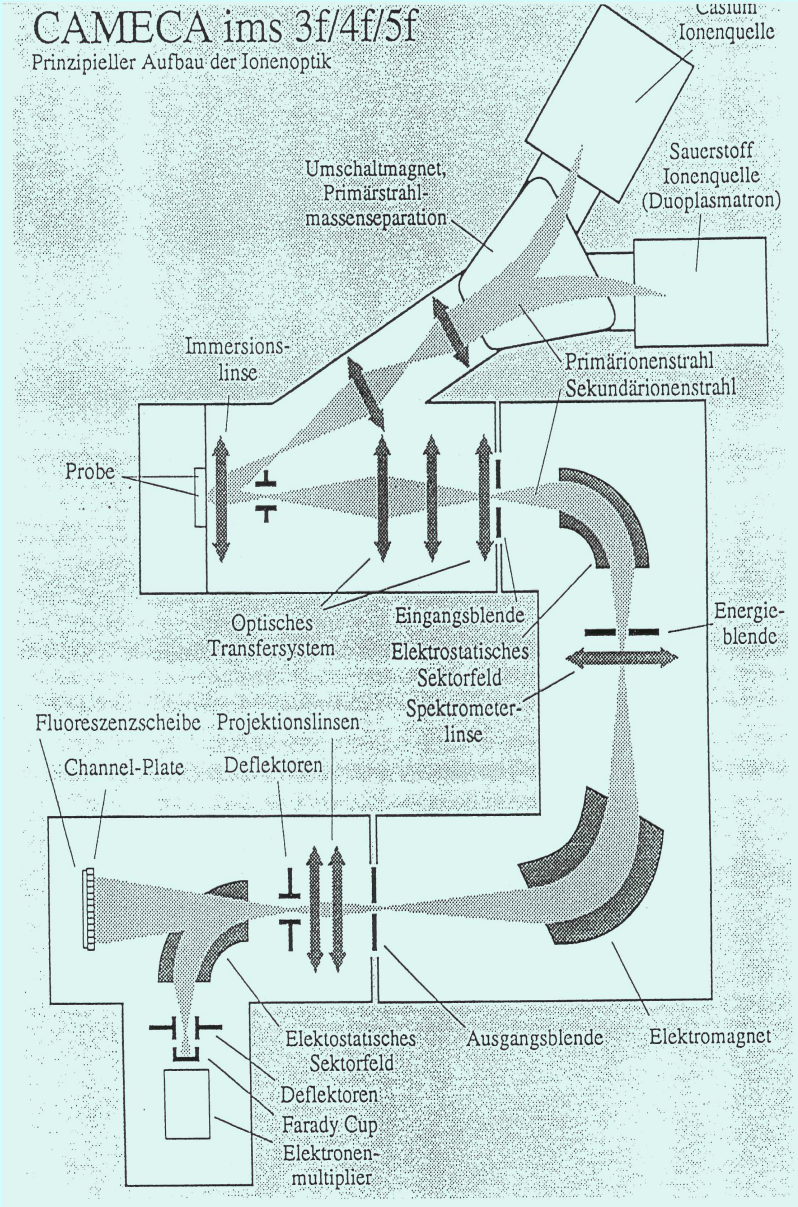

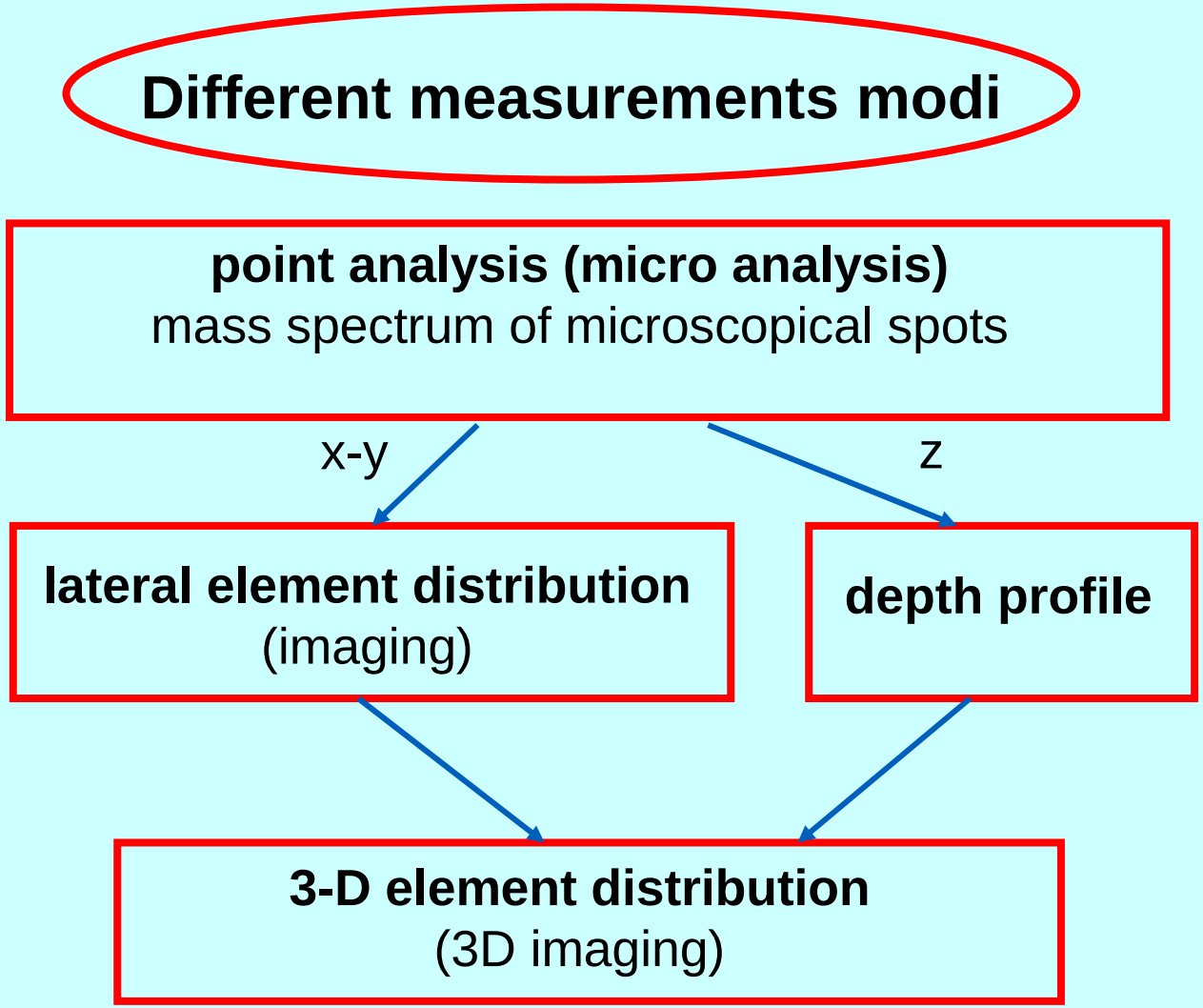
Different measurements modi
point analysis (micro analysis)
mass spectrum of microscopical spots
x-y
z
lateral element distribution
(imaging)
depth profile
3-D element distribution
(3D imaging)

different beam modi

Point measurement

Line measurement

Scanning modus

Point resolution is determined by the diameter of the beam spot.
It figures out about 1-3 micrometer.

The scanned area is tipically between 150 und 250 μm^2

Small beam spots result in decreased element sensitivity
because of the low ionic currents.

Limit of detection

is determined by the interaction between:

spot diameter
layer thickness
ionic current
} volume

For example:

limit	spot	depth	volume
1 ppm	1 μm	1000 nm	0.785 μm^3
1000 ppm	1 μm	1 nm	0.000785 μm^3
1 ppm	10 μm	10 nm	0.785 μm^3

depth profile:

sputtering process → sputtering time
SIMS crater → depth

The time to depth conversion is difficult because of the preferential sputtering process (NRA is here in advantage).

depth resolution:

Theoretically just a couple of atomic rows, in practice 5-10 nm because of the roughness of the samples
(comparable with RBS)

SIMS mass spectrum

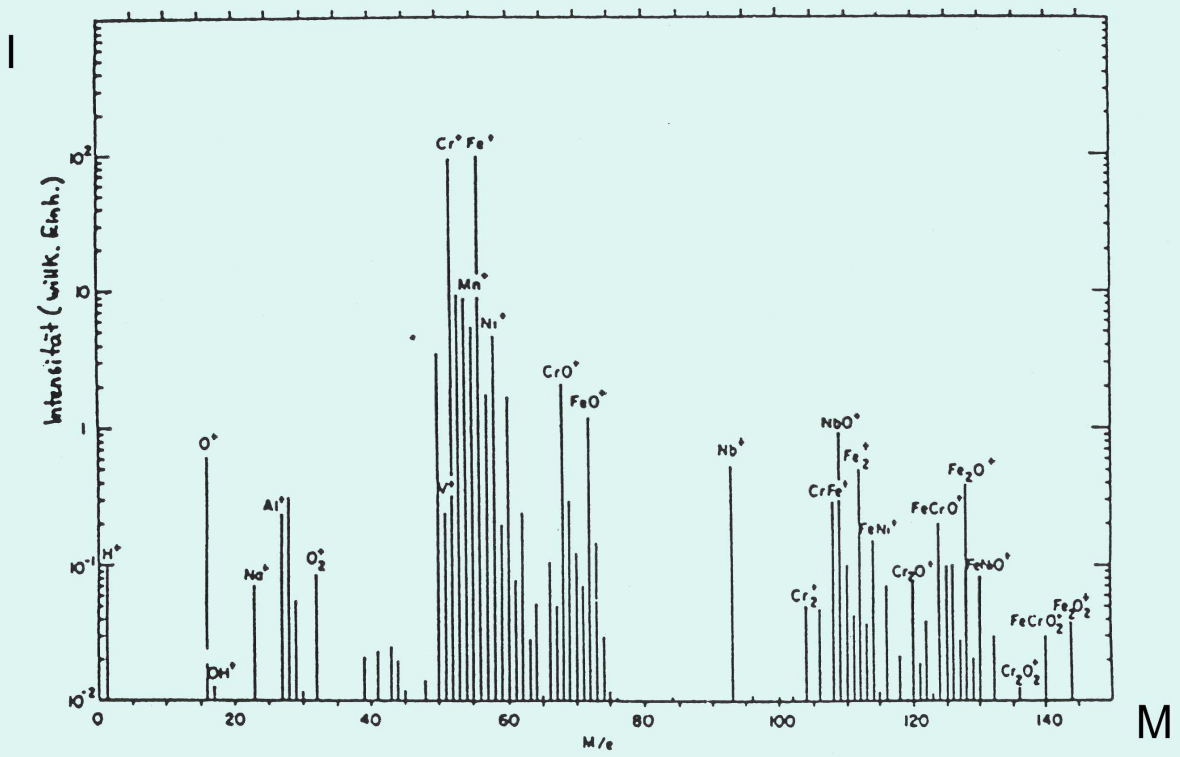

Some applications

depth profile of H in Si

concentration of B in Si

Al depth profile in GaAs multilayer

comparison between SIMS und RBS measurements in Si/CoSi/Co_2Si/Co thin film sample

Ti-diffusion in Ni-Zr-Al sample

O-diffusion in PZT ferroelectrics

Depth profile of implanted H in Si.

The maximum of the H peak is in a depth of 550 nm.

surface peak

SIMS

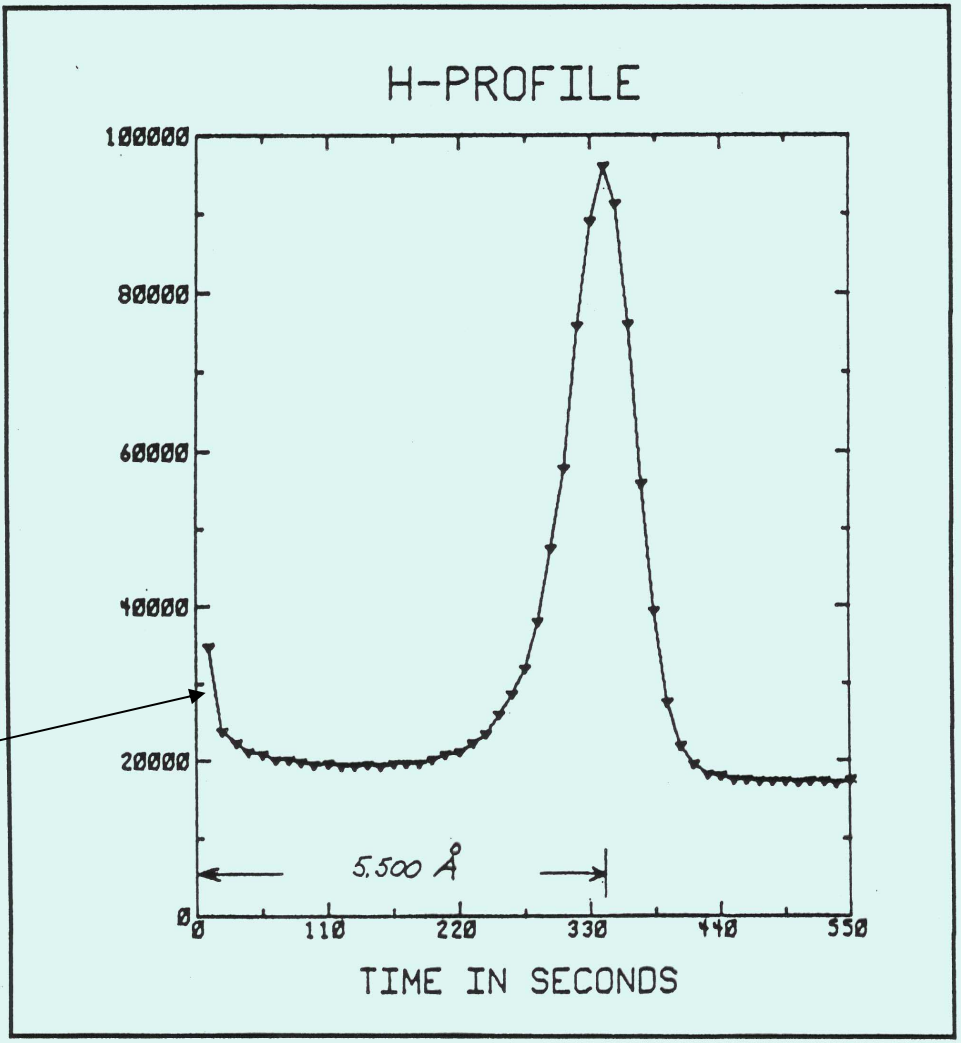

H-Tiefenprofile in Si

B in Si

The concentration profile of B was determined between 10^{16} and 10^{20} atom/cm^3 over 4 ordner of magnitude

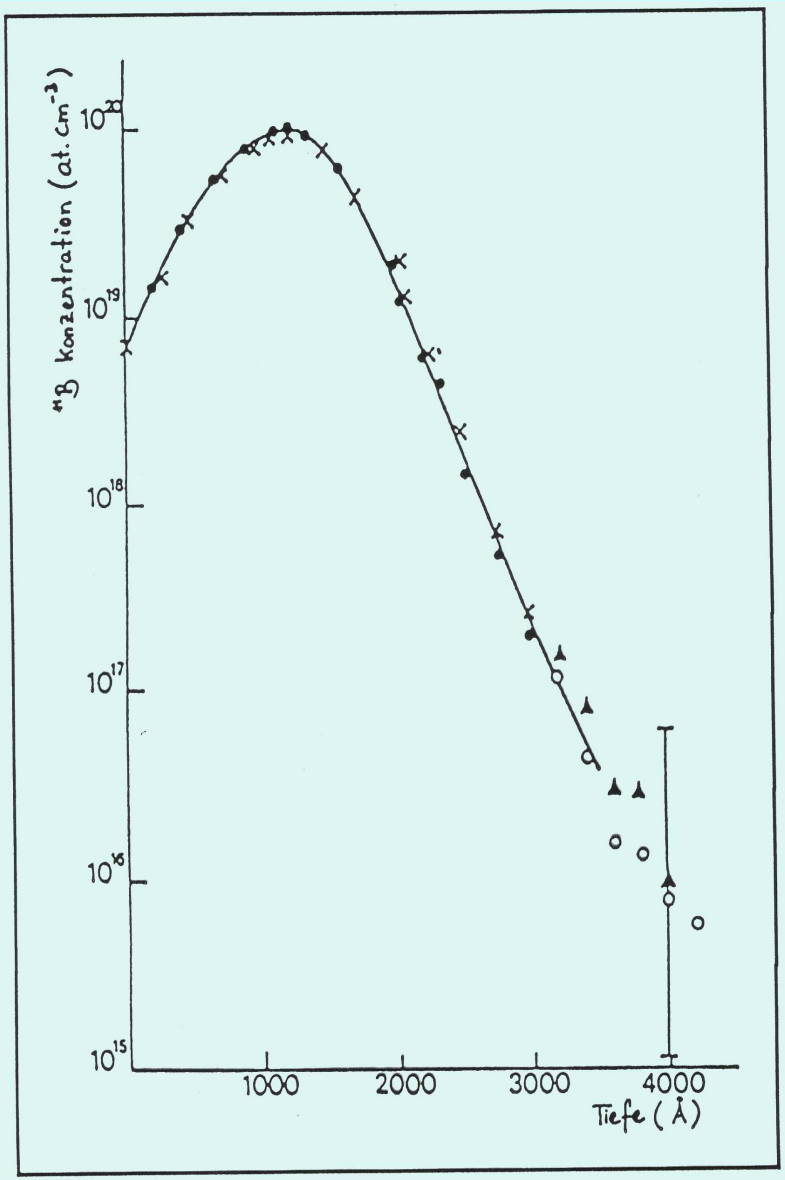

Monitoring of Al in a GaAs thin film system

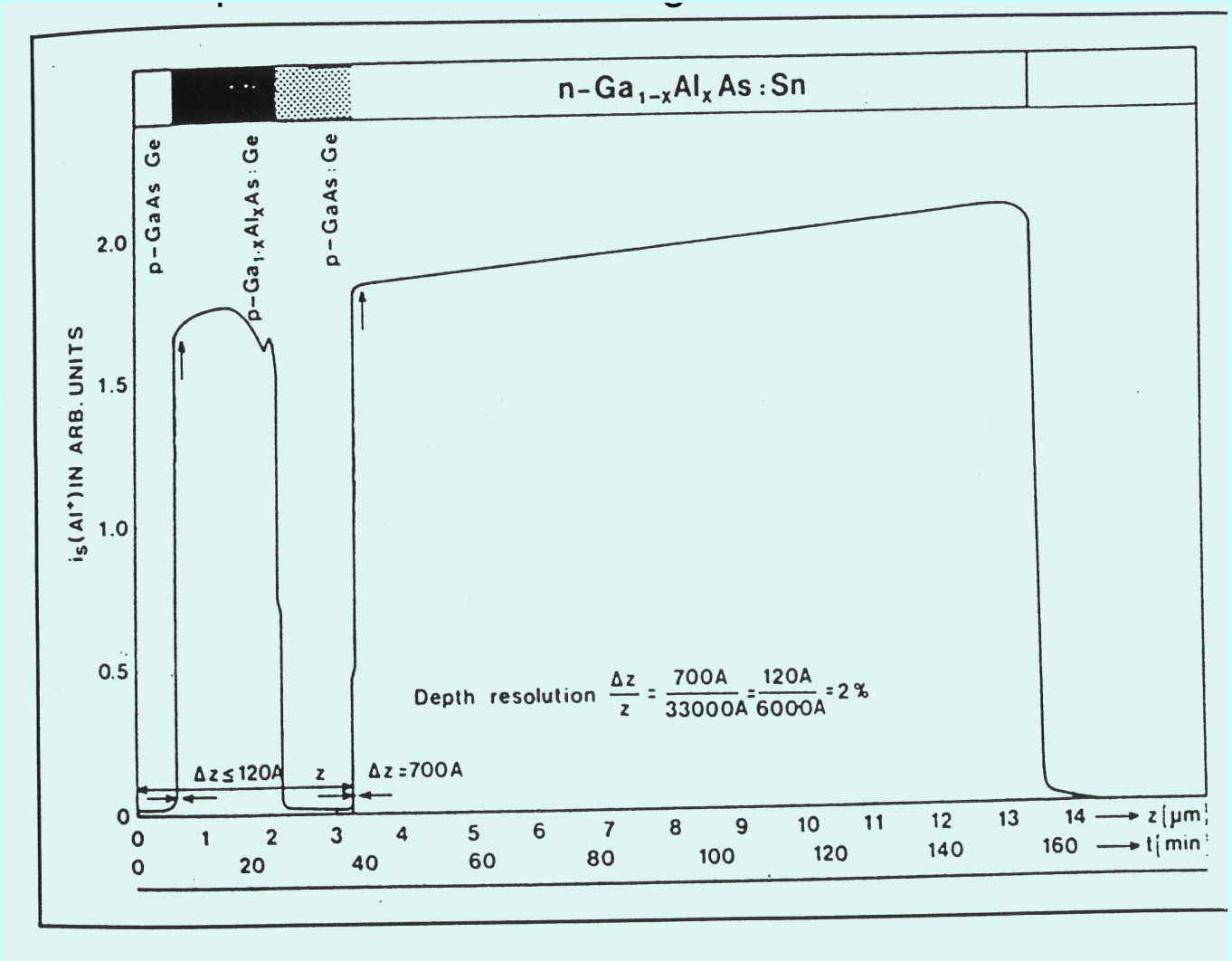

Comparison between RBS and SIMS spectra of a $Co/Co_2Si/CoSi/Si$ thin film sample

RBS

SIMS

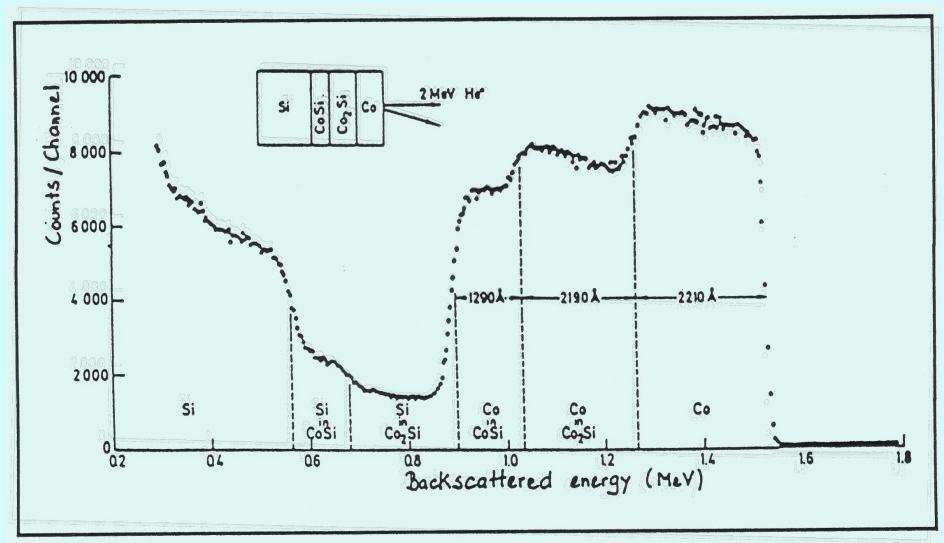

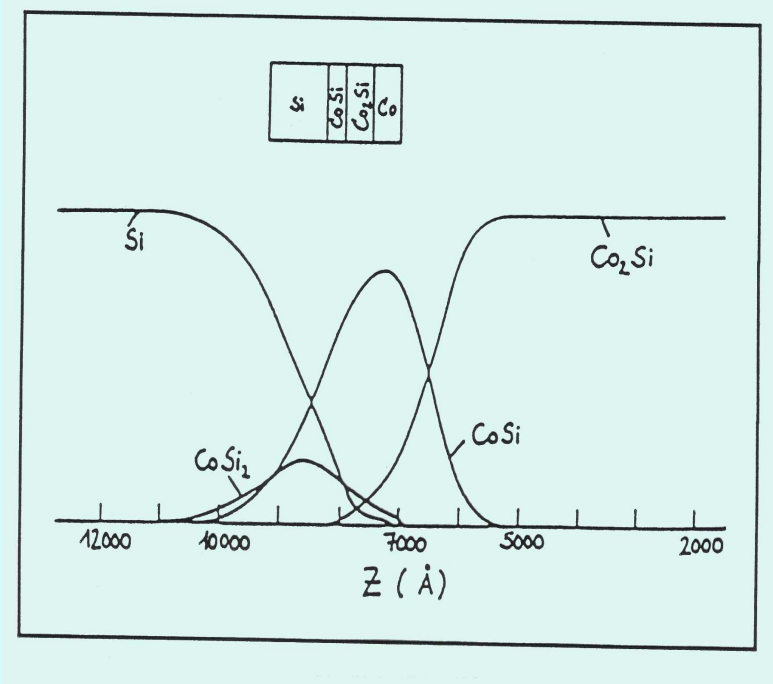

Ti-diffusion in a $Ni_{23}Zr_{62}Al_{15}$ sample

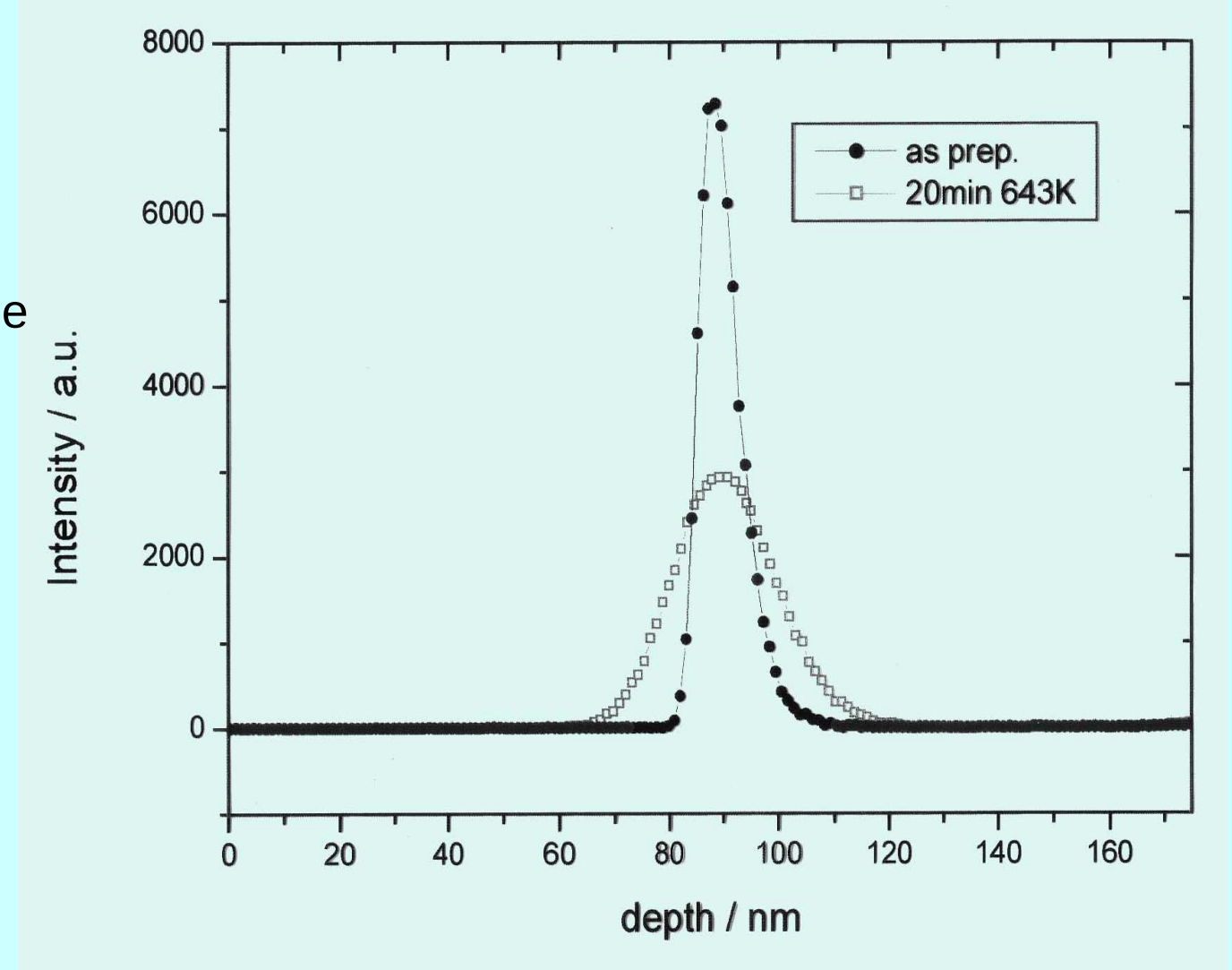

^{18}O depth profile in PZT (Pb-Zr-Ti-O) ferroelectric samples

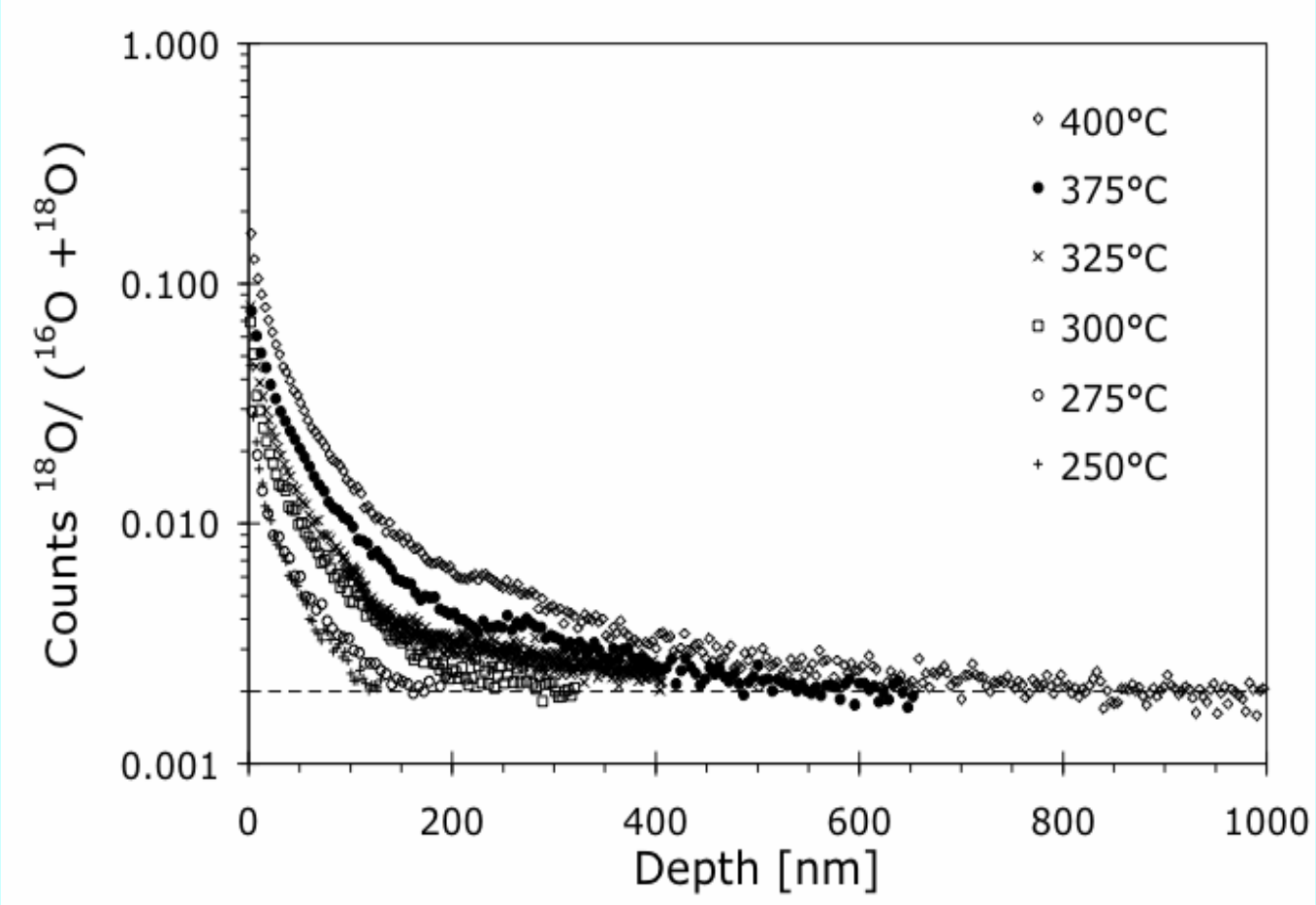

Particle Induced X-Ray Emmission/ Proton Induced X-ray Emission (PIXE)

Principle of proton induced x-ray emission

First step:
electrons from the inner shells (frequently K-electrons) will be kicked out by primary protons with a tipical energy of 1-2 MeV.

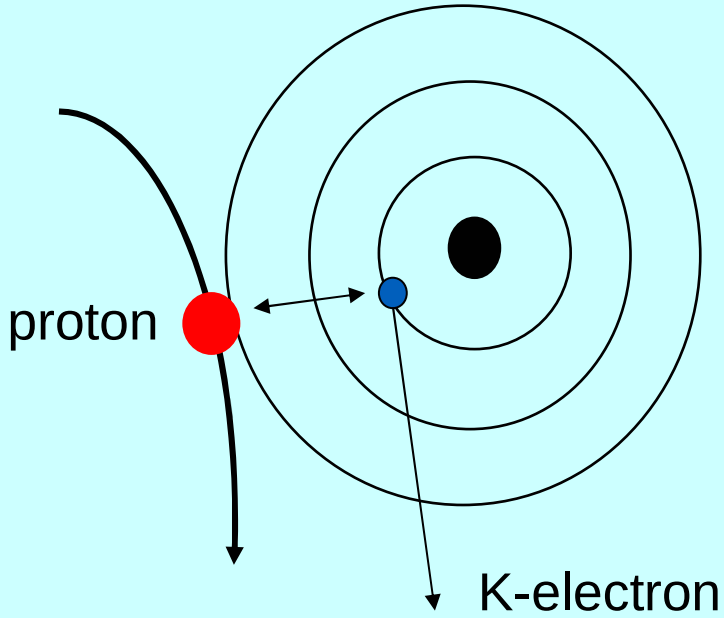

second step:
the electron hole will be filled up by electrons from higher shells.
Hereby characteristic x-ray emission with element specific frequency and concentration dependent intensity will be created.

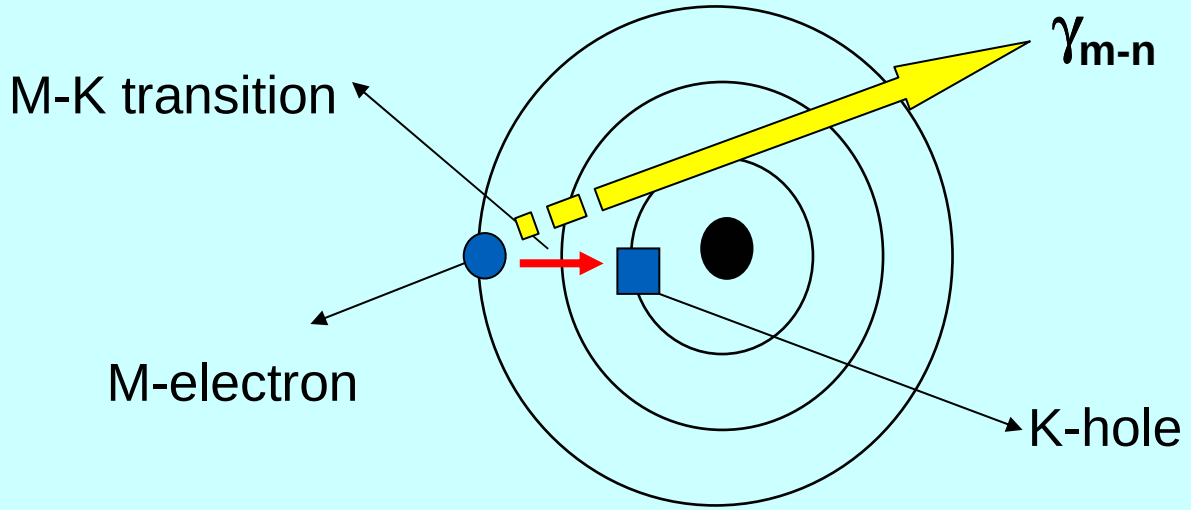

$$E = h\nu \Rightarrow \nu_{m-n} = \frac{E_m - E_n}{h} = \frac{2\pi^2 m_e^2 e^4}{h}\left(\frac{1}{m^2} - \frac{1}{n^2}\right)$$

important features:

excellent sensitivity (about one order of magnitude better as of the electron micro probe)

poor depth resolution, because x-ray emission has to be detected

good lateral mapping of trace elements if combined with a proton micro beam

non-destructive

Why is the sensitivity so excellent?

The reason is the strong reduction in the background, which is caused by the bremsstrahlung. Bremsstrahlung has a continuous energy distribution and will be produced always if electrons will be slowed down by a solid.

$$I(\text{Bremsstrahlung}) \approx \frac{1}{M(\text{projectile})} \Rightarrow I^{BS}_{protons} << I^{BS}_{electrons}$$

As a consequence, the sensitivity of PIXE is much more better than of EMPA

some applications

biology	trace element analysis
enviromental research	air pollution
archeology	analysis of ancient paintings and coins
ion microscope	combined with strongly focused ion beam, laterale mapping of trace elements and multi element analysis

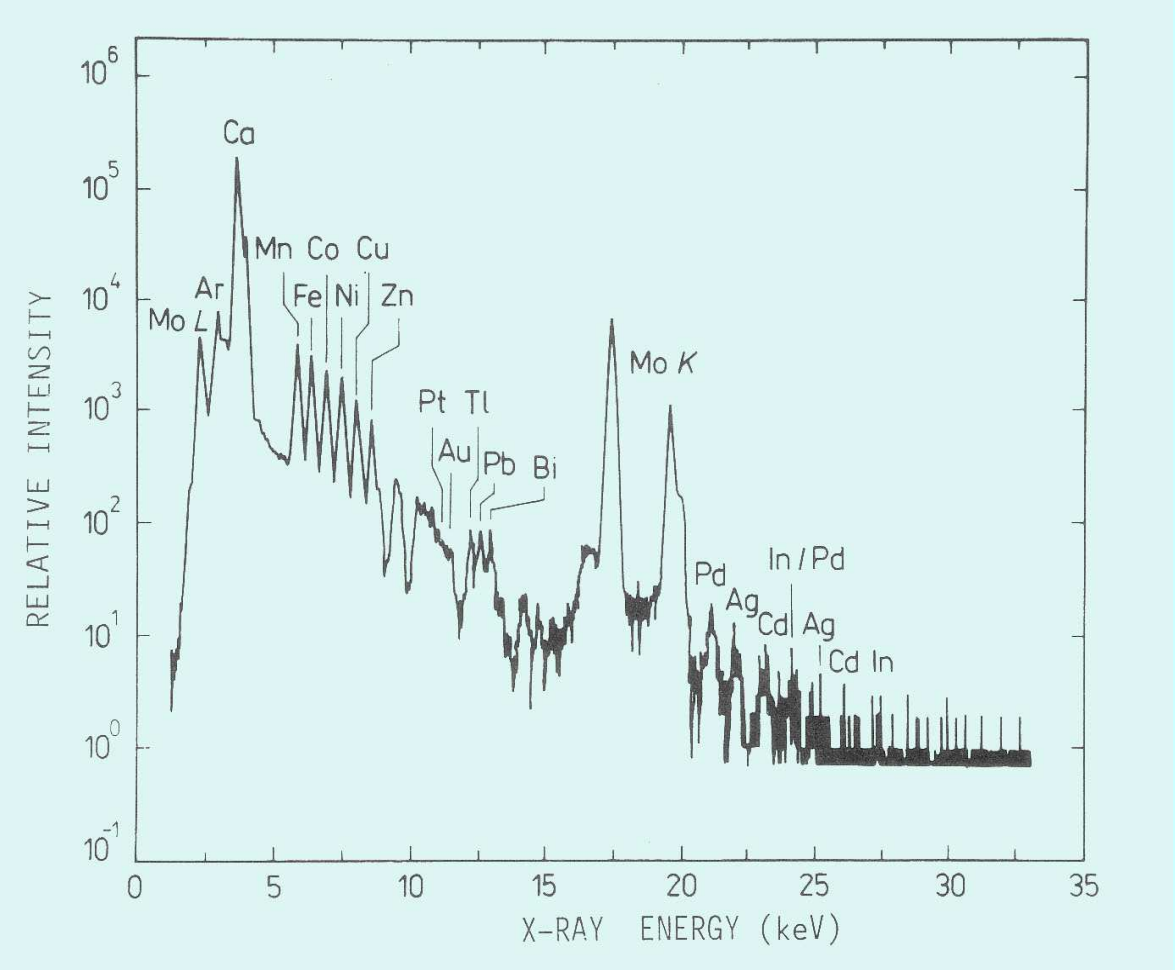

PIXE spectrum of an aqueous sample containing only 10µg of each of the investigated elements

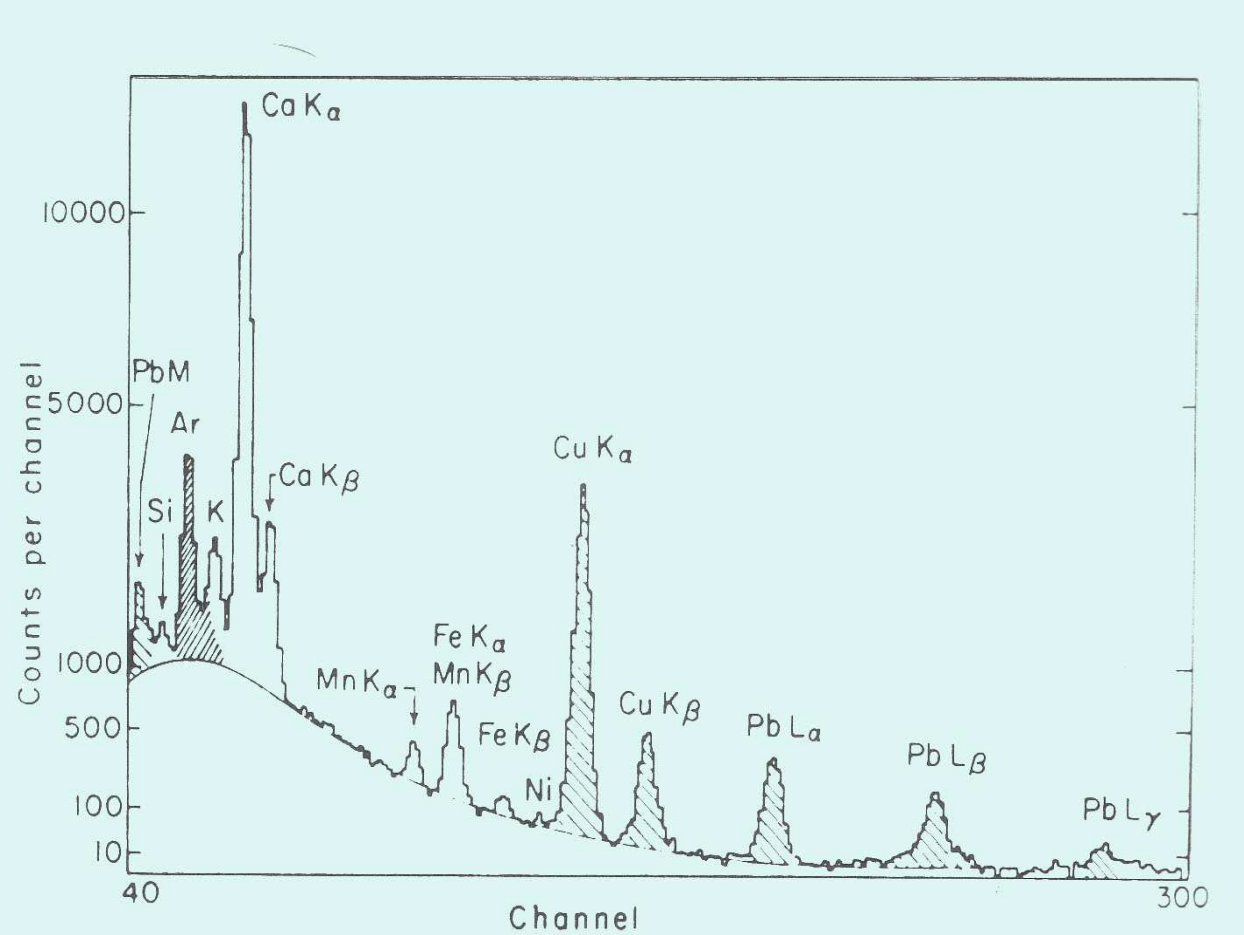

X-ray spectrum of ink on paper from the Gutenberg Bible

Elastic Recoil Detection Analysis

ERDA

principle of the method

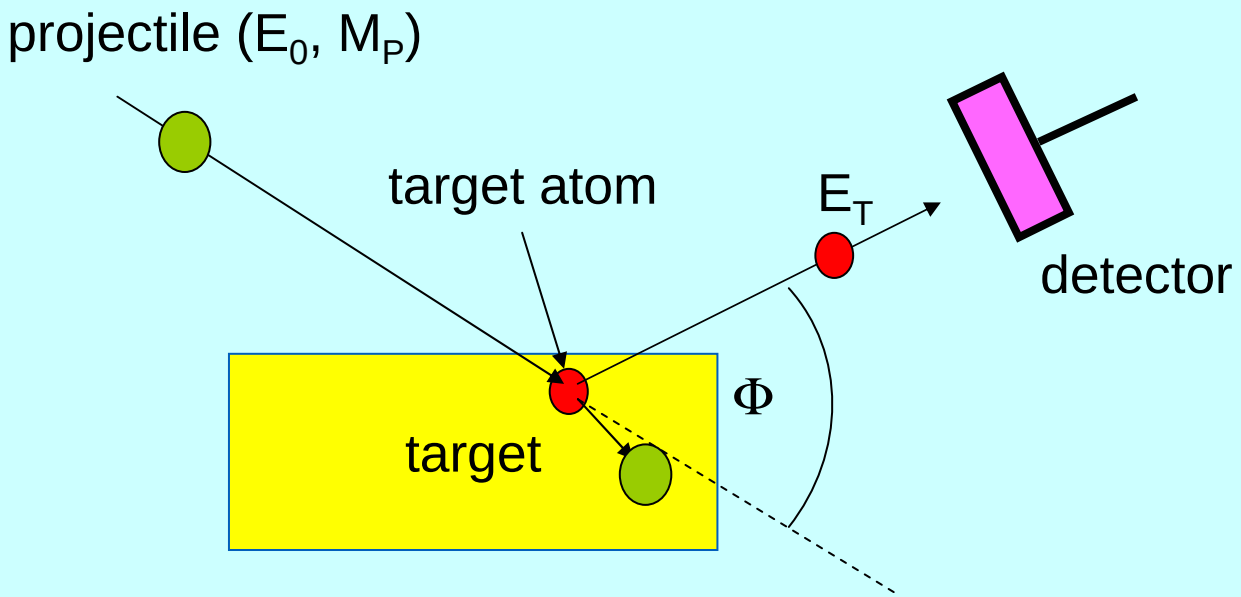

$$K_{ERDA} = \frac{E_T}{E_0} = \frac{4\left(M_P / M_T\right)}{\left[1+\left(M_P / M_T\right)\right]^2}\cos^2\Phi$$

The method is similar to an RBS measurement, however, instead of the backscattered primary ions the kicked out target atoms will be detected. This results in the direct detection of the target atoms and herewith the determination of the composition of the target. Also the enrgy of the detected target atoms will be measured, therefore, similarily to RBS, depth profiles can be defined.

The transfered energy has to be high in order to make it possible that a target atom will be kicked out from the sample. Therefore, heavy projectile are necessary, that will be scattered on the lighter target atoms $M_P > M_T$.

For ERDA measurements generally an energy of about 1 MeV/amu is necessary. In order to detect lighter target atoms like H, He, Li, N, C, O ($Z<9$), one has to use heavyer projectiles like Si, Cl or Ar correspond to an energy of 30-40 MeV. Furthermore it is possible to measure also H isotopes using a He beam.

benefits of the method:

simple measuring technique
direct detection of target atoms
qualitative and quantitative analysis

disadvantages:

dept resolutuion is poorer
sensitivity is poorer

Development of the method: time of flight (TOF) ERDA:
measurement of velocity (time) and energy of atoms

TOF ERDA set-up

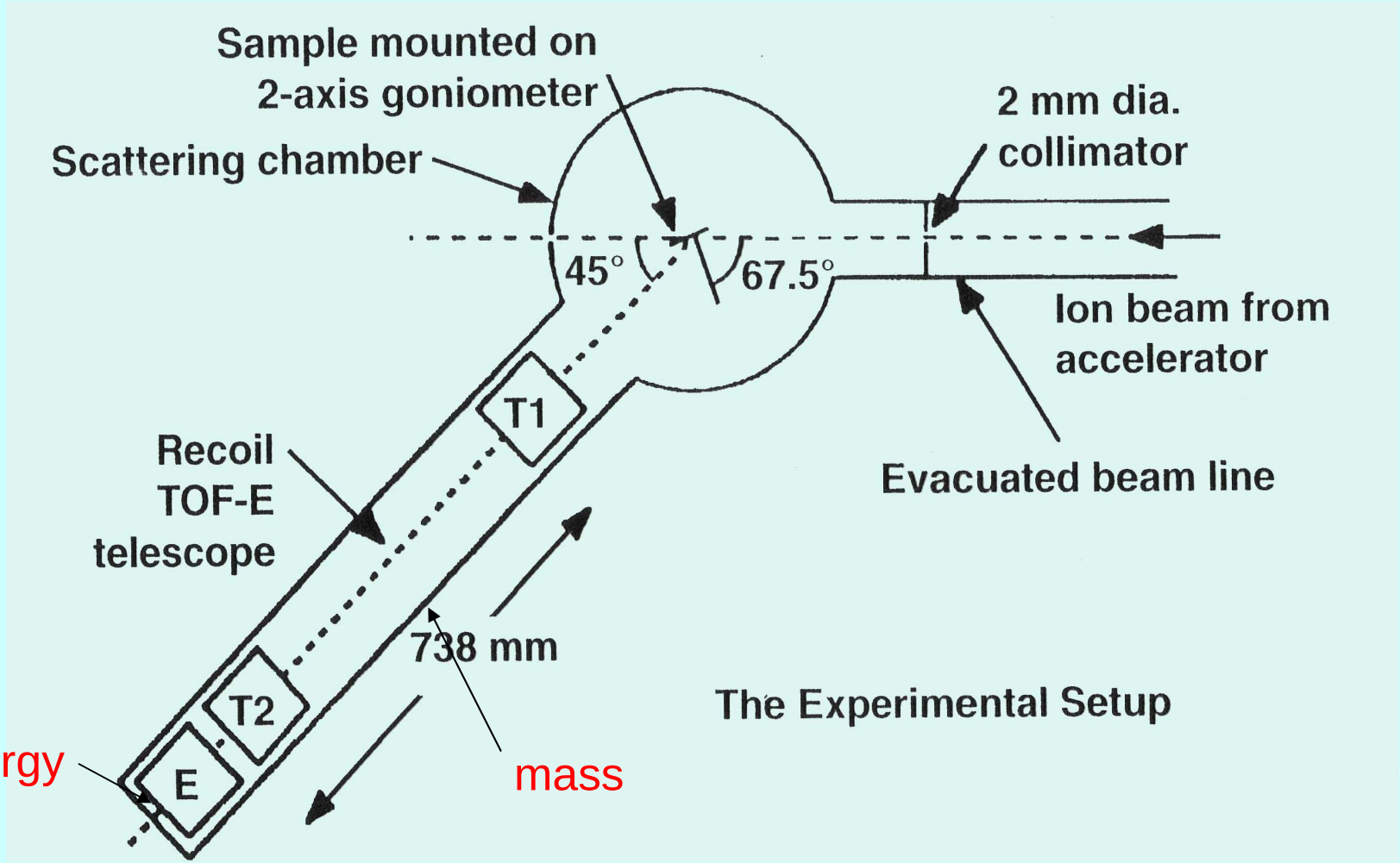

Comparison of ERDA and RBS geometry

Straggling ~ Z_1^2

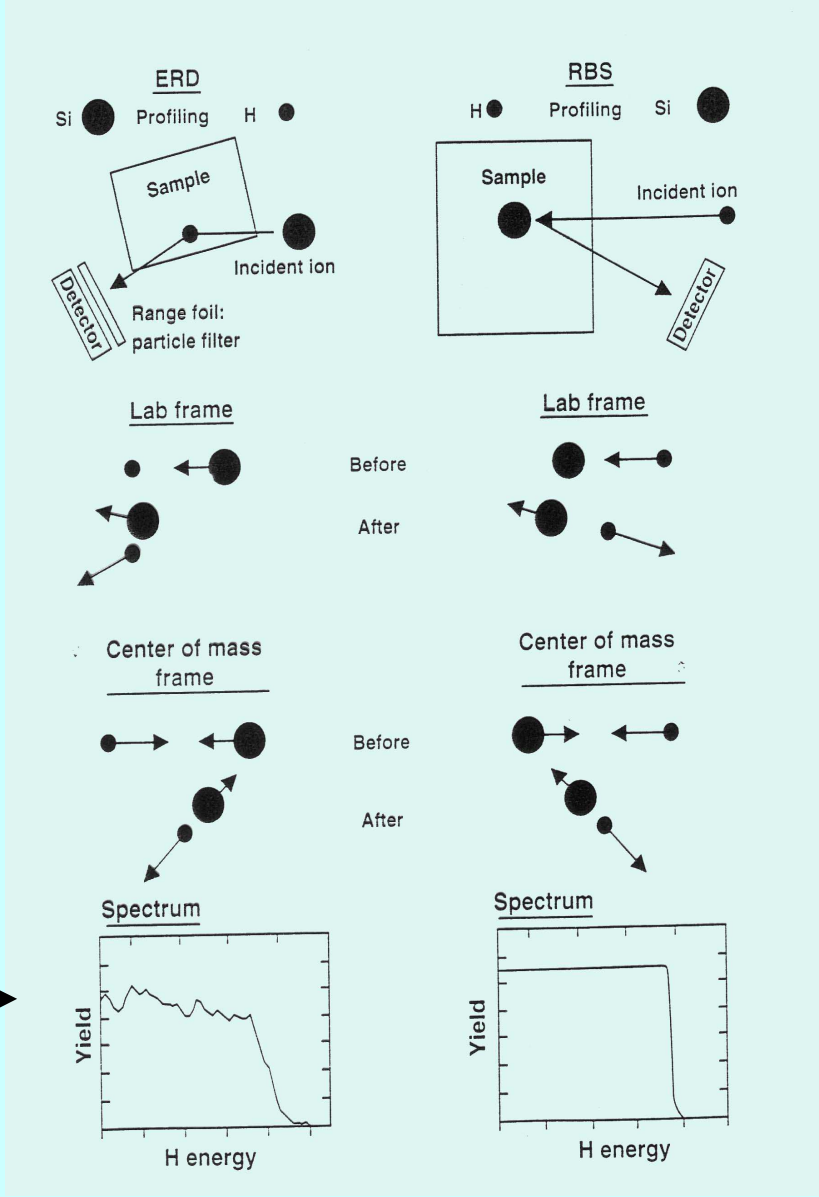

detection of H and Li in a $LiNbO_3$ sample using Si projectiles

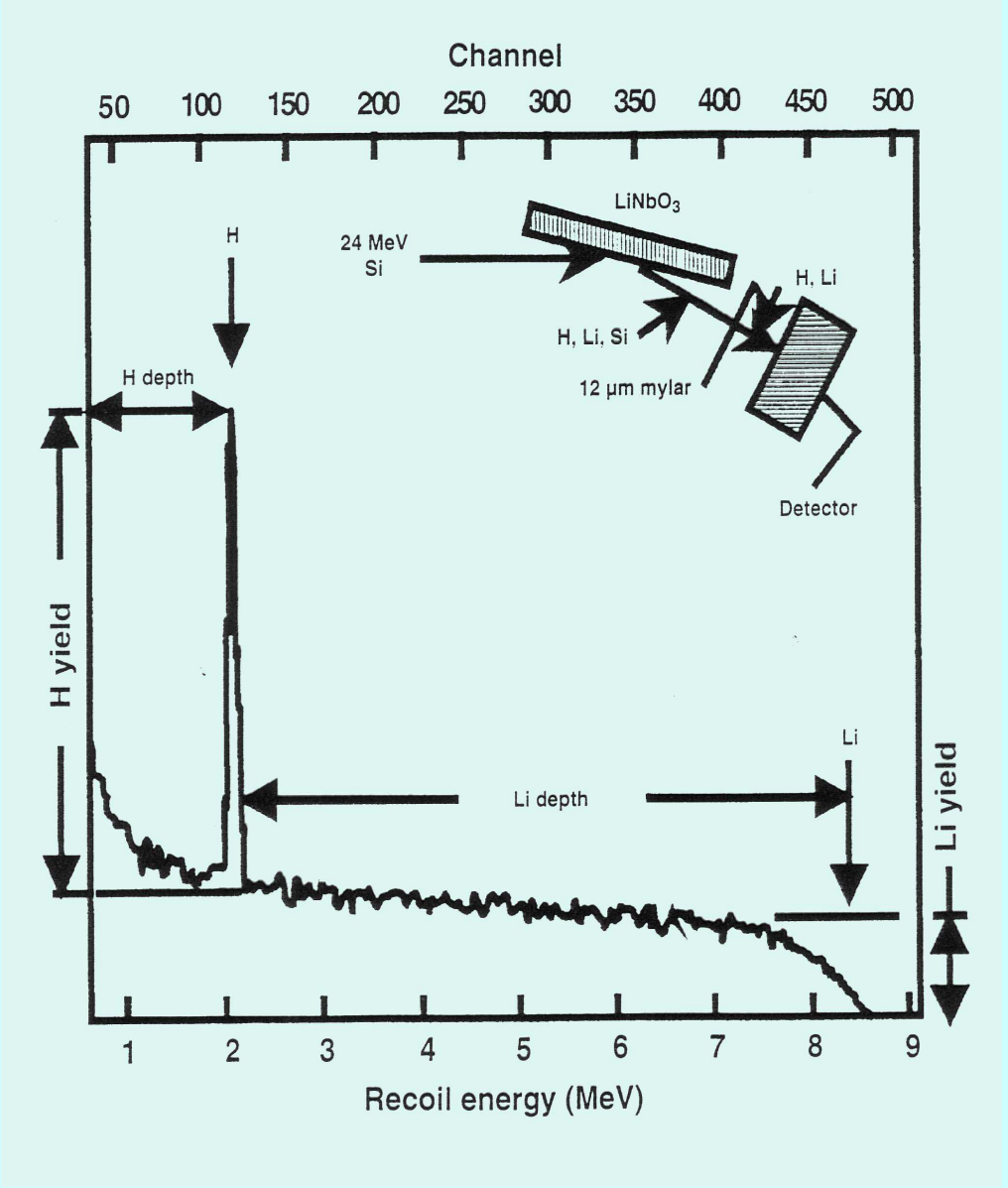

Detection of H and D in a thin polymer film using He projectils

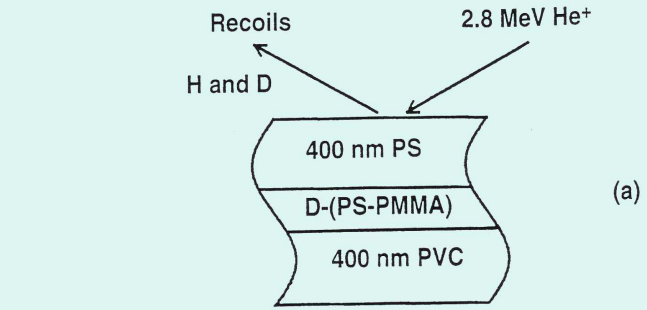

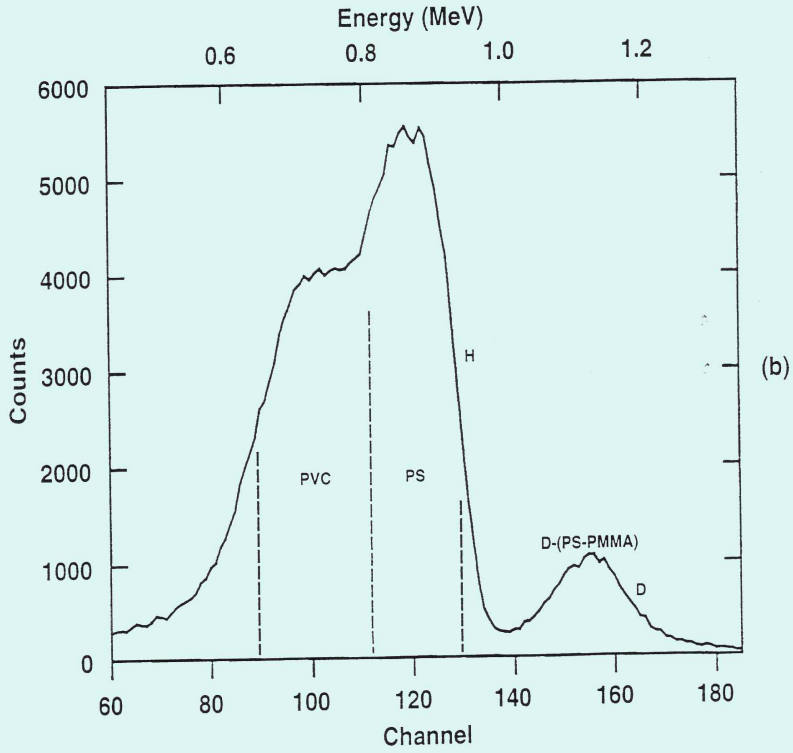

Concentration depth profiles of H and D

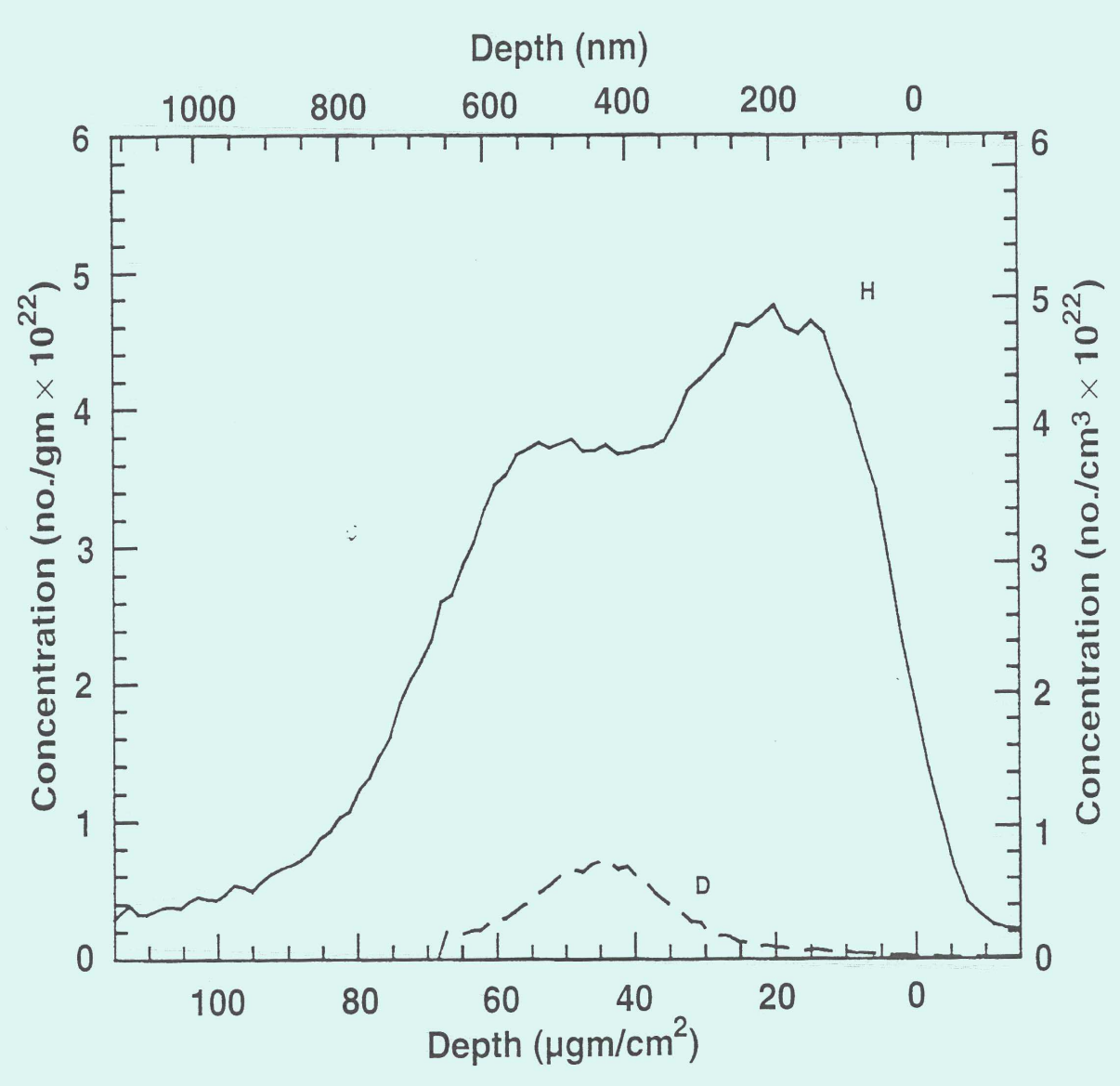

3D view of light elements measured using Au projectiles in a TOF ERDA set-up

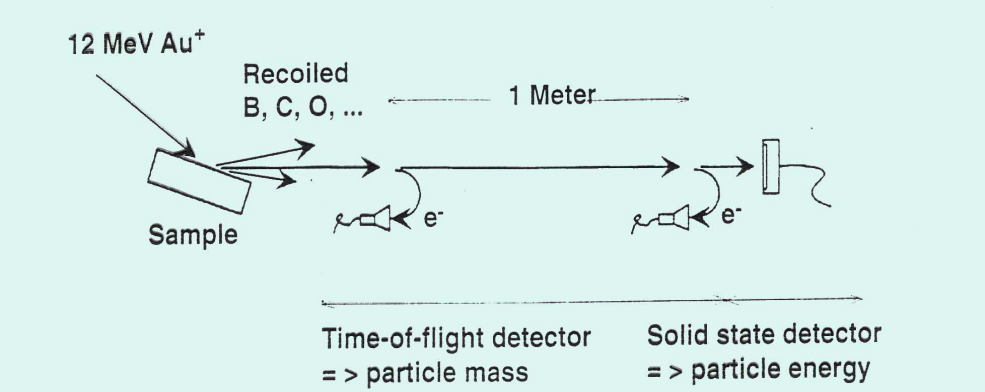

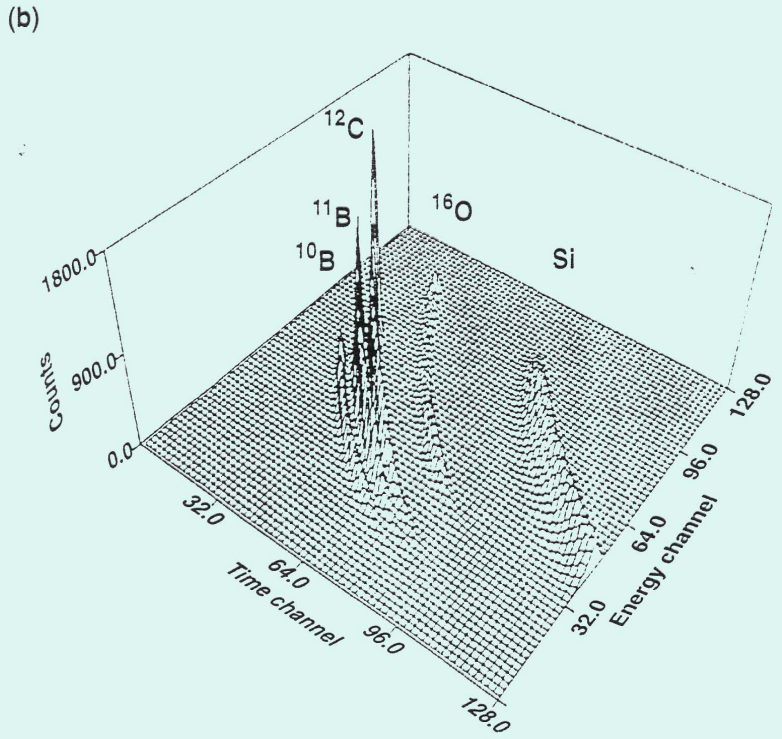

Concentration depth profiles of B, C and O

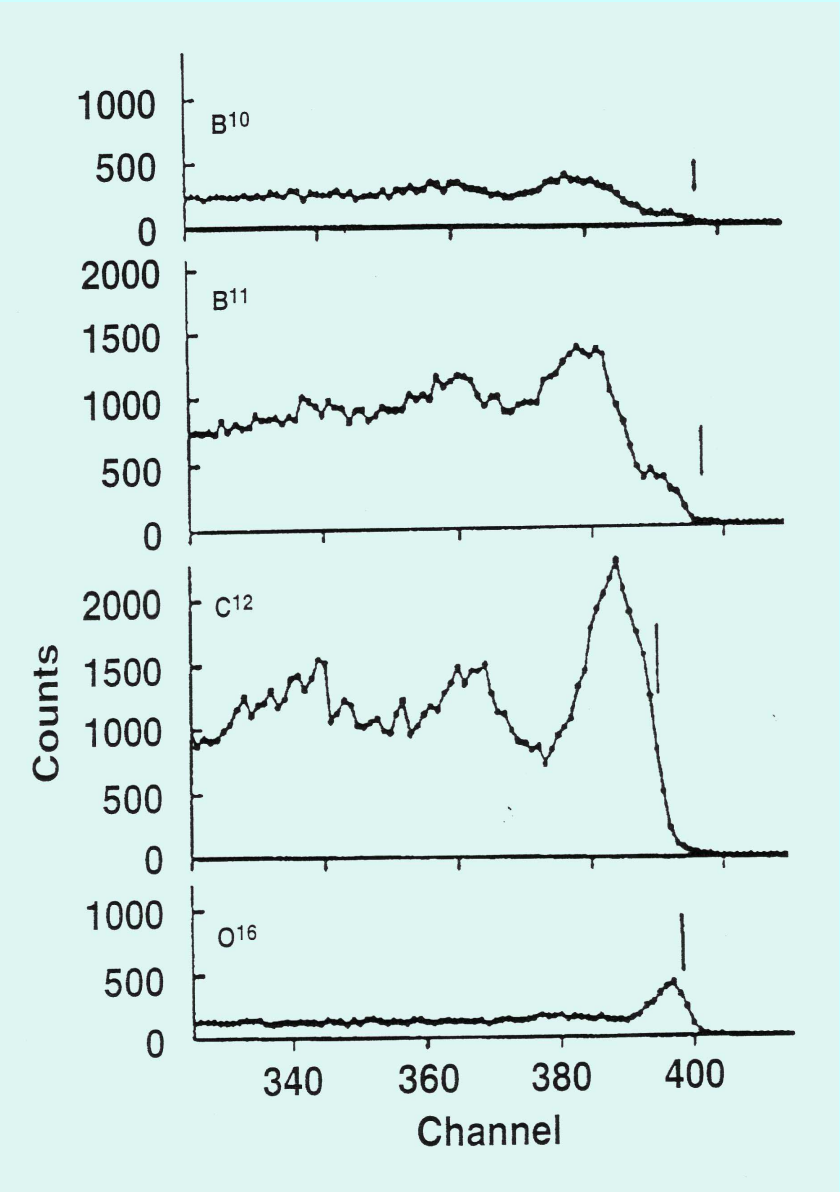

N profiling in a SiN sample

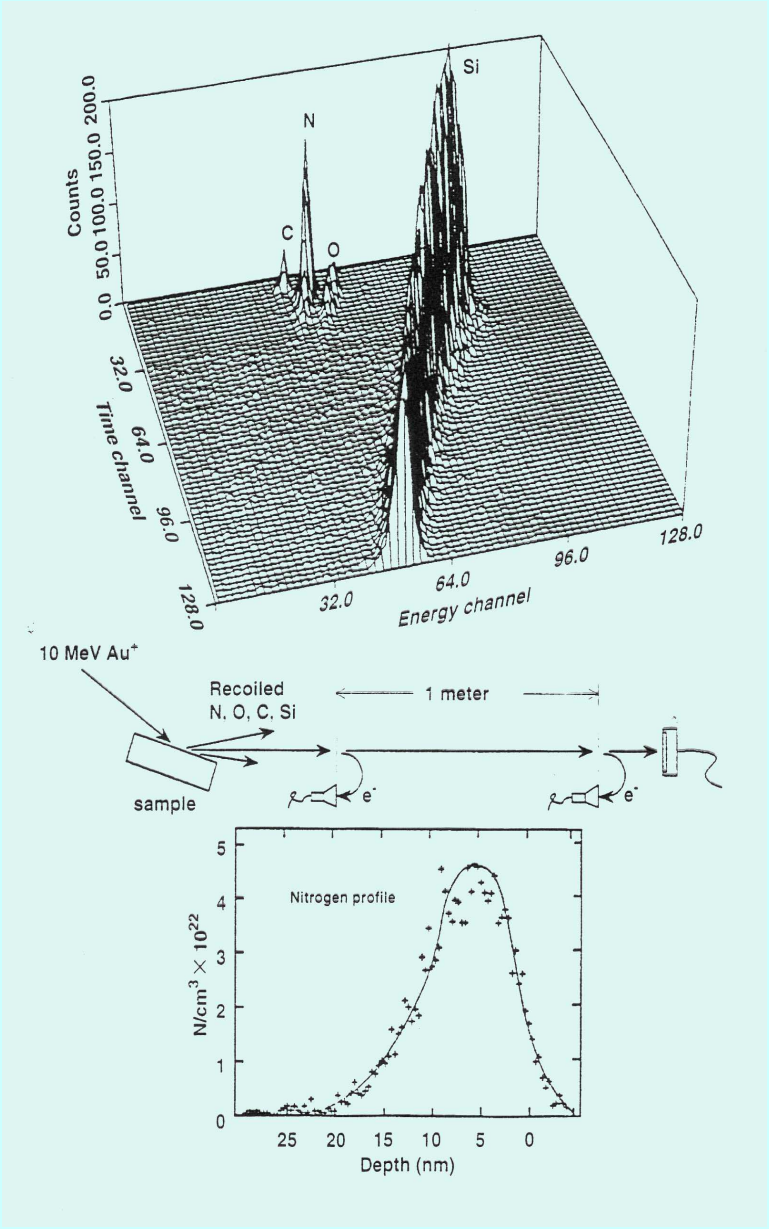

Sensitivity of different analytical methods for surface analysis as a function of atomic number in an interference free situation

ESCA: electron spectroscopy for chemical analysis

LIMS: laser ionization mass spectroscopy

SIMS: secondary ion mass spectroscopy

RBS: Rutherford backscattering spectrometry